AFRL-SN-RS-TR-2006-69
In-House Interim Report
March 2006

TERAHERTZ (THZ) IMAGING

APPROVED FOR PUBLIC RELEASE; DISTRIBUTION UNLIMITED.

AIR FORCE RESEARCH LABORATORY
SENSORS DIRECTORATE
ROME RESEARCH SITE
ROME, NEW YORK

STINFO FINAL REPORT

This report has been reviewed by the Air Force Research Laboratory, Information Directorate, Public Affairs Office (IFOIPA) and is releasable to the National Technical Information Service (NTIS). At NTIS it will be releasable to the general public, including foreign nations.

AFRL-SN-RS-TR-2006-69 has been reviewed and is approved for publication

APPROVED: /s/

WILLIAM J. BALDYGO
Chief, Radar Signal Processing Branch
Sensors Directorate

FOR THE DIRECTOR: /s/

RICHARD G. SHAUGHNESSY
Chief, Rome Operations Office
Sensors Directorate

REPORT DOCUMENTATION PAGE

Form Approved
OMB No. 074-0188

1. AGENCY USE ONLY (Leave blank)	2. REPORT DATE	3. REPORT TYPE AND DATES COVERED
	MARCH 2006	In-House Interim, SEP 04 – AUG 05

4. TITLE AND SUBTITLE
TERAHERTZ (THZ) IMAGING

5. FUNDING NUMBERS
C - N/A
PE - 62704F
PR - 517R
TA - 15
WU - 00

6. AUTHOR(S)
Raghuveer Rao

7. PERFORMING ORGANIZATION NAME(S) AND ADDRESS(ES)
Air Force Research Laboratory/SNRT
26 Electronic Parkway
Rome New York 13441-4514

8. PERFORMING ORGANIZATION REPORT NUMBER
N/A

9. SPONSORING / MONITORING AGENCY NAME(S) AND ADDRESS(ES)
Air Force Research Laboratory/SNRT
26 Electronic Parkway
Rome New York 13441-4514

10. SPONSORING / MONITORING AGENCY REPORT NUMBER
AFRL-SN-RS-TR-2006-69

11. SUPPLEMENTARY NOTES
AFRL Project Engineer: Dr Braham Himed/SNRT/(315) 330-2551/ Braham.Himed @rl.af.mil

12a. DISTRIBUTION / AVAILABILITY STATEMENT
APPROVED FOR PUBLIC RELEASE; DISTRIBUTION UNLIMITED.

12b. DISTRIBUTION CODE

13. ABSTRACT ***(Maximum 200 Words)***
Previously, the problem of Concealed Weapon Detection, CWD, was addressed in the context of detecting weapons concealed under clothing. Infrared and millimeter wave images were considered for the purpose. Infrared detection depends on the concealed weapon's temperature being significantly different from that of its surroundings. Millimeter wave detection relies on reflection from the object of interest. Passive detection is possible in many instances since MMW is present naturally and can penetrate various types of clothing. Active devices can also be used to provide MMW illumination. It was found that IR images are less reliable since one can easily defeat or mask the object's response. MMW detector technology has only now advanced to the point where real time images are possible. Imaging in the Terahertz (THz) wavelengths was an avenue that suggested itself as worthy of exploration. Like MMW it penetrates clothing. However, with wavelengths ranging from 1 micron to 1 mm, it provides superior resolution. Furthermore, it offers spectroscopic capability that enables object identification not only by shape attributes but also by material composition. This opens up applications such as standoff detection of explosives. The range of 300 GHz to 3 THz has been explored by many researchers. Standoff ranges of up to 50 meters can be achieved at these frequencies. The main limitation is water vapor absorption. A considerable amount of work has been done in developing THz generators and detectors. However, there is much work that needs to be done in the area of signal and image processing algorithms for making THz technology useful in applications such as CWD and explosives detection.

14. SUBJECT TERMS
Concealed Weapon Detection (CWD), Infrared (IR), Millimeter Wave (MMW), Terahertz (THZ) Imaging.

15. NUMBER OF PAGES
53

16. PRICE CODE

17. SECURITY CLASSIFICATION OF REPORT	18. SECURITY CLASSIFICATION OF THIS PAGE	19. SECURITY CLASSIFICATION OF ABSTRACT	20. LIMITATION OF ABSTRACT
UNCLASSIFIED	UNCLASSIFIED	UNCLASSIFIED	UL

Table of Content

Acknowledgment

The support and collaboration of Braham Himed, Michael Wicks, Jerry Genello, Bill Baldygo, Joshua Markow and Domenico Luisi are gratefully acknowledged. The author is thankful to Dr. Robert Bowman for making the IPA possible at the Rochester Institute of Technology end. The assistance of Sujay Narayanswamy, graduate student at RIT, in pointing to references was valuable.

1. Background

The assignment came about with the main aim of developing new thrusts for the Air Force Research Laboratory, Sensors Directorate, Radar Signal Processing Branch (SNRT) with strong ties to security applications such as perimeter surveillance, concealed weapon detection (CWD) and related problems. My own previous work in image processing for CWD and other security-related imaging with visual, x-ray, infrared and millimeter wave imagery was seen as a jumping-off point for identifying new areas. The IPA agreement listed the following as *anticipated roles*:

1. To define key research problems in homeland security that are amenable to solution in a scientific framework.
2. To initiate a research program to investigate all or a subset of the problems identified.
3. To interface with the Department of Homeland Security and other agencies for transitioning of research product for actual use.
4. To ensure that the program becomes self-sustaining with potential to contribute over the next decade.
5. Items 1 and 2 have largely been fulfilled and efforts are under way in regards to items 3 and 4.

2. Identification of Opportunity

A substantial part of the early effort was devoted to identifying the most appropriate new thrust. Several different possibilities were considered including sensor networks, new evolutionary programming based optimization techniques and signal processing for concealed object detection and classification. A detailed evaluation of the state of the art of these different fields was performed. New innovations in the first two fields are much more tied to generic communication and architectural problems than to a direct addressing of the problem of detecting and classifying threats. On the other hand, the third area addresses the security and surveillance problem directly and is well in line with SNRT's technical interests.

We have previously addressed the problem of CWD in the context of detecting weapons concealed under clothing. Infrared and millimeter wave images were considered for the purpose. Infrared detection depends on the concealed weapon's temperature being significantly different from that of its surroundings. Millimeter wave (MMW) detection relies on reflection from the object of interest. Passive detection is possible in many instances since MMW is present naturally and can penetrate various types of clothing. Active devices can also be used to provide MMW illumination. Examples of our prior work in enhancing such images are found in [1]. It was found that Infrared (IR) images are less reliable since one can easily defeat or mask the object's response. MMW detector technology has only now advanced to the point where real time images are possible.

Imaging in the Terahertz (THz) wavelengths was an avenue that suggested itself as worthy of exploration. Like MMW it penetrates clothing. However, with wavelengths ranging from 1 micron to 1 mm, it provides superior resolution. Furthermore, it offers spectroscopic capability that enables object identification not only by shape attributes but also by material composition [2]. This opens up applications such as standoff detection of explosives [3]. The range of 300 GHz to 3 THz has been explored by many researchers. Standoff ranges of up to 50 meters can be achieved at these frequencies. The main limitation is water vapor absorption. There is huge interest in the potential of THz technology. A considerable amount of work has been done in developing THz generators and detectors. However, there is much work that needs to be done in the area of signal and image processing algorithms for making THz technology useful in applications such

as CWD and explosives detection. The next section will provide an overview of THz imaging.

3. THz Technologies

Although a precise definition of the Terahertz region does not exist, a commonly accepted range is the 300 GHz to 3 THz region [4]. This corresponds to wavelengths of 100 μm to 1 mm. This has been a relatively unexplored region of the electromagnetic spectrum and has been referred to as the "Terahertz gap." The gap has had mostly to do with the lack of source and detector technologies until recently. For Electro-Magnetic (EM) radiation with wavelengths longer than the THz, antenna and waveguide technologies have been available for several decades whereas for shorter than THz wavelengths, optica,l and optoelectronic technologies have been used. The two technologies have to be brought together to generate and study the THz region, which is also referred to as the far infrared.

Some of the earliest works that invoke the term Terahertz are in acoustics in the context of photon generation [5, 6]. The occurrence of THz bandwidths in the context of high pressure CO_2 laser operation was predicted in [7]. Explicit reference to a device as a potential detector of THz radiation occurs in [8]. Synthesis of terahertz radiation has been made possible by the development of three distinct approaches [9, 10]:

1. Direct emission from far-infrared incoherent sources,
2. Up-conversion from microwave frequencies to terahertz frequencies.
3. Down-conversion of coherent lasers operating in the near infrared to the terahertz band.

The optically driven sources exhibit more power at terahertz frequencies than direct emission or up-conversion. A typical arrangement for pulsed THz generation is shown in the context of time domain spectroscopy as shown in Figure 1. A light pulse from the femtosecond laser source strikes a device (shown separately in Figure 2) which essentially consists of electrodes embedded in a Gallium Arsenide (GaAs) substrate. A Direct Current (DC) bias is maintained across the electrodes. The current discharge due to ionization of the dielectric from the laser pulse results in the generation of a free space THz pulse. The same device works as a detector in reverse. Instead of maintaining a DC bias, wires are led away from the electrodes. When a THz pulse strikes the substrate in synchronization with a light pulse, a current pulse is generated in the wires.

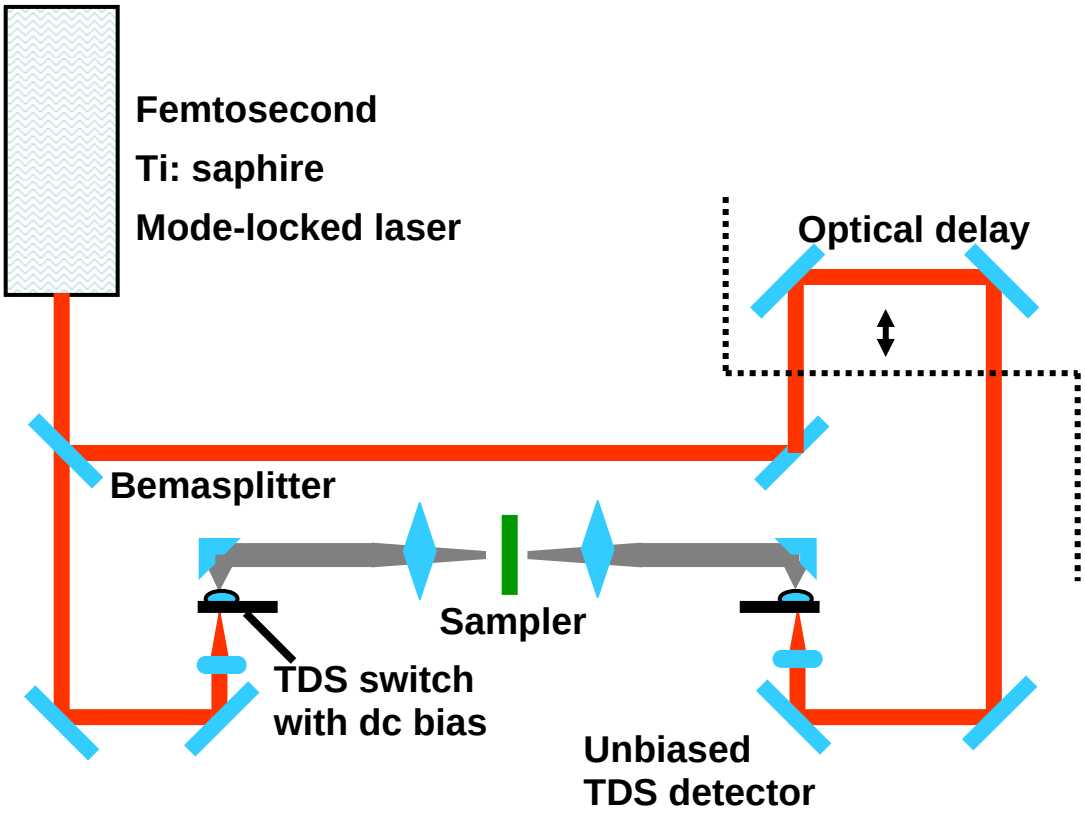

Figure 1. THz time-domain spectroscopy using pulsed THz generation. After Eric Mueller [10].

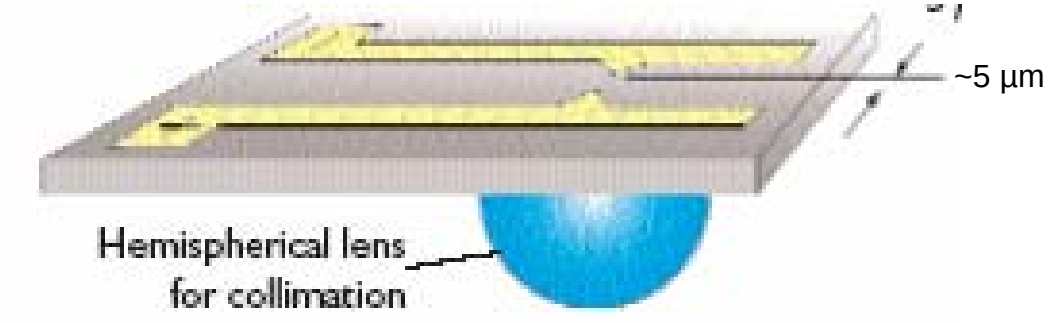

Figure 2. THz generation device. After Eric Mueller [10].

The attributes of various methods of THz generation are summarized in Table 1 [10].

Table 1. Properties of THz generation methods

		Generation Method			
		Optically pumped THz lasers	**Time-domain spectroscopy**	**Direct multiplied sources**	**Frequency mixing**
Attribute	**Average power**	> 100 mW	~ 1 μW	mW - μW	< 1 μW
	Frequency range	0.3 to 10 THz	0.1 to 2 THz	01. To 1 THz	0.3 to 10 THz
	Tunability	Discrete steps	N/A	10 to 15% of center	Continuous
	Mode	CW / Pulsed	Pulsed	CW	CW

3.1 Time-Domain Spectroscopy

The arrangement in Figure 1 can be used to perform time-domain spectroscopy (TDS). The optical delay shown in the figure is used to adjust the time instant of sampling THz radiation from the detector. The material sample, whose THz spectral response is to be obtained, is positioned in the path of the generated THz pulse and the output is sampled at the detector at different instants. If the THz pulses are generated in periodic fashion, the optical delay can be adjusted to gate the detector at different instants in the period. The samples at the various instants can be used to construct a time-domain profile of the response of the material. A Fourier transformation of the profile provides the spectral response of the material in the THz regime. An image can be generated by optical scanning of the input beam or by moving the sample around. THz TDS is by no means confined to transmission data. It is possible to get reflective data from samples by slight alteration of the detector path in Figure 1.

3.2 Terahertz Tomography

The fact that full field measurements, that is, phase and magnitude measurements are available with THz makes reflection tomography possible [11]. In principle, range calculations are made by comparing the phase of THz reflections with the phase of the

transmitted THz signal. The range map as a function of position allows for reconstruction of the surface of the object in three dimensional (3D). The range measurements can be made with either pulsed or continuous wave THz waveforms. A version of tomographic reconstruction resembling seismic migration is proposed in [12]. As shown in Figure 3, pulses sent from transmitter T are received after reflection at layer boundaries by multiple receiver elements R. Delay and sum operations are performed to reconstruct reflection intensity at various points.

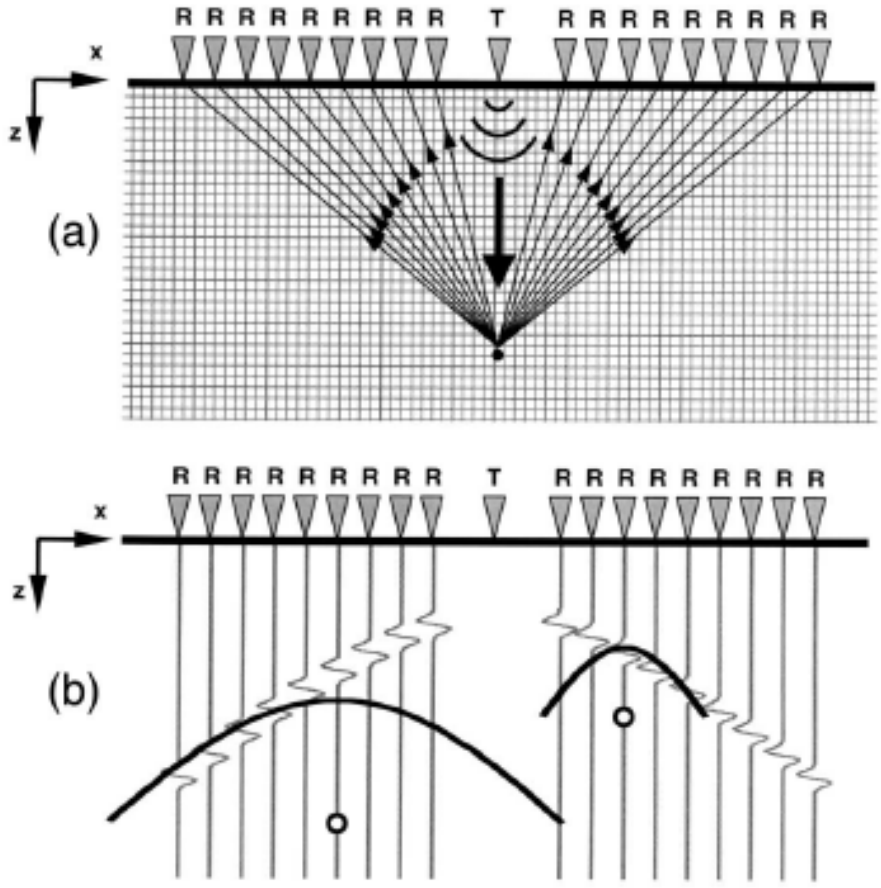

Figure 3. Multistatic reflection imaging. From Dorney et al [12].

4. Perspective and Summary of Accomplishments

Figure 4 summarizes our perspective of the components required for successful development of THz imaging. It involves the confluence of three entities: signal processing, photonics, and electronics.

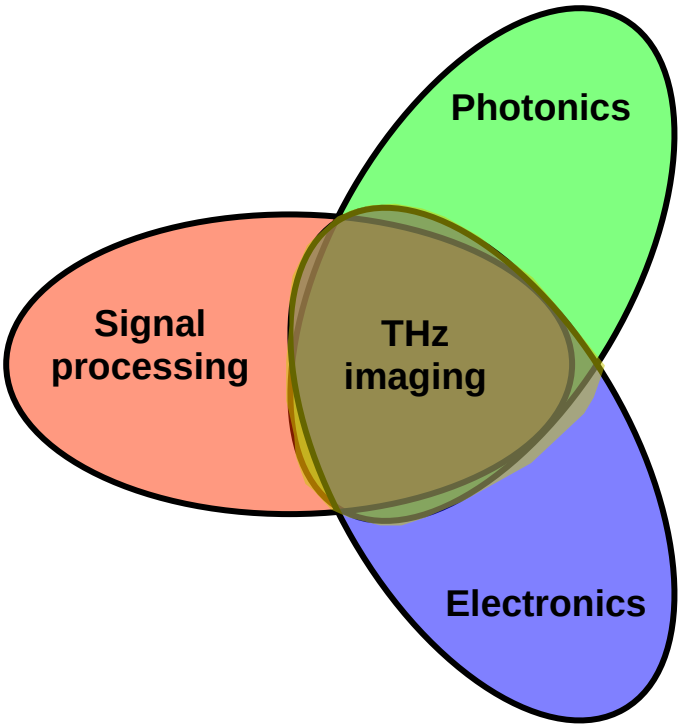

Figure 4. Components of THz imaging

Clearly a lot of effort has been invested in the photonics and electronics areas through the development of generation and detection technologies. The area that is least developed is signal processing of THz data. In this regard, the key accomplishments of the assignment have been the following:

1. Key signal processing issues that need to be addressed for significant improvement in THz imaging have been identified and potential lines of investigation have been proposed.
2. Preliminary mathematical formulation and simulation results have been obtained for signal processing problems in THz image reconstruction.

Focal plane detector arrays are not yet available in the usual operating range of 0.3 to 5 THz. Antenna array based imaging using signal processing techniques is therefore an

attractive alternative. We have developed mathematical formulation and preliminary solutions for correlative interferometric image reconstruction problems with antenna arrays. Computer simulations have also been performed for tomographic reconstruction of complex-valued projections using MATLAB phantoms. The next section details the investigation into correlative interferometry.

5. Imaging through Correlative Interferometry

The construction of THz images of extended objects using correlative interferometry has been proposed by Federici and colleagues [13]. The key advantages of this approach are:

1. It works even with incoherent radiation.
2. Synthetic aperture techniques can be used to reduce the number of actual detectors used.

Researchers in this field suggest that improvement to the synthesized data can be done with techniques such as the CLEAN algorithm and the Maximum Entropy Method (MEM) that have been widely used in radio astronomy. Our view is that such techniques are oriented towards point sources and scatterings. Furthermore, the CLEAN algorithm requires at least the first identified peak to be a true fully resolved isolated component. We propose developing constrained optimization methods that offer super-resolution potential.

5.1 Correlative interferometry in the far-field

Suppose $f(\theta)\cos\left[2\pi ft+\varphi(\theta)\right]$ is the far-field electric field amplitude at $x=0$ of the EM wave with direction of arrival θ (see Figure 5).

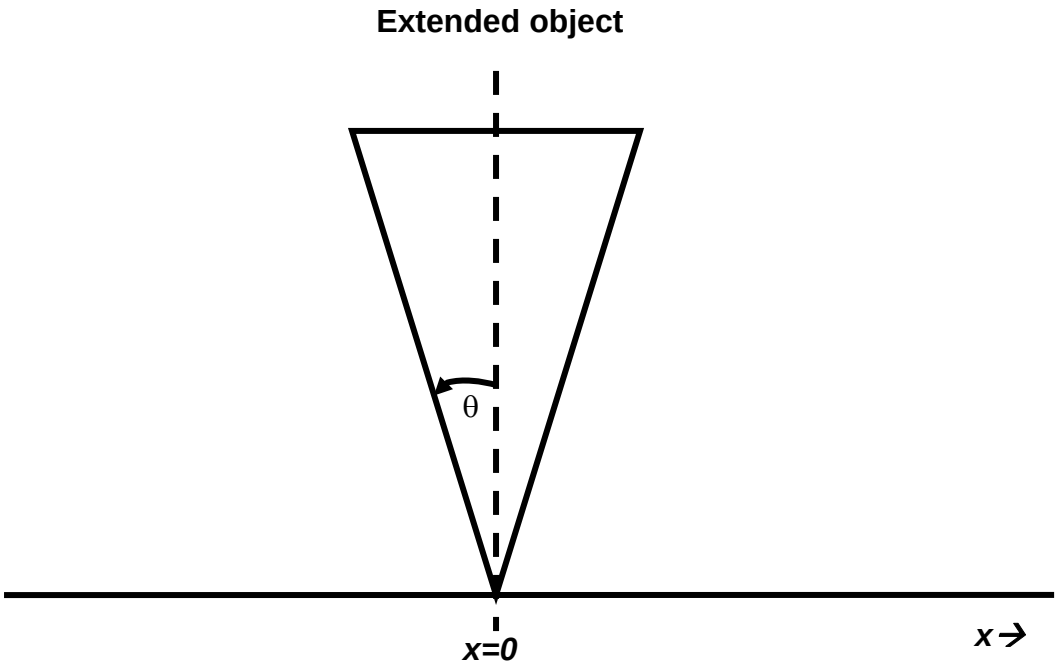

Figure 5. Object viewed in far field

Then, the contribution of the field covering an elemental angle $d\theta$ in the neighborhood of this angle to the field at x is equal to

$$f(\theta)\cos\left[2\pi f\left(t-\frac{x}{c}\sin\theta\right)+\varphi(\theta)\right]d\theta. \tag{1}$$

The total field $F(x)$ at x is equal to an integration of the above over all angles and is given by

$$\begin{aligned} F(x) &= \int_{-\pi/2}^{\pi/2} f(\theta)\cos\left[2\pi f\left(t-\frac{x}{c}\sin\theta\right)+\varphi(\theta)\right]d\theta \\ &= \int_{-\pi/2}^{\pi/2} f(\theta)\cos\left[2\pi ft-\frac{2\pi x}{\lambda}\sin\theta+\varphi(\theta)\right]d\theta \end{aligned}. \tag{2}$$

The cross-correlation $R(x,y)$ between the fields at two distinct points x and y is given by

$$R(x,y)=E\{F(x)F(y)\}=$$

$$E\left\{\int_{-\pi/2}^{\pi/2}\int_{-\pi/2}^{\pi/2} f(\theta)\cos\left[2\pi ft-\frac{2\pi x}{\lambda}\sin\theta+\varphi(\theta)\right]f(\mu)\cos\left[2\pi ft-\frac{2\pi y}{\lambda}\sin\mu+\varphi(\mu)\right]d\theta\,d\mu\right\}. \tag{3}$$

Equation (3) can be written as

$$E\{F(x)F(y)\}=\frac{I_1+I_2}{2} \tag{4}$$

where

$$I_1=E\left\{\int_{-\pi/2}^{\pi/2}\int_{-\pi/2}^{\pi/2} f(\theta)\,f(\mu)\cos\left[\frac{2\pi x}{\lambda}\sin\theta-\frac{2\pi y}{\lambda}\sin\mu+\varphi(\mu)-\varphi(\theta)\right]d\theta\,d\mu\right\}$$

and

$$I_2=E\left\{\int_{-\pi/2}^{\pi/2}\int_{-\pi/2}^{\pi/2} f(\theta)\,f(\mu)\cos\left[4\pi ft-\frac{2\pi x}{\lambda}\sin\theta-\frac{2\pi y}{\lambda}\sin\mu+\varphi(\theta)+\varphi(\mu)\right]d\theta\,d\mu\right\}.$$

If we have incoherent radiation and assume that $\varphi(\theta)$ is uniformly distributed between $-\pi$ and π with $\varphi(\theta)$ and $\varphi(\mu)$ independent for $\theta\neq\mu$, we have

$$R(x,y)=I_1(x,y)=\int_{-\pi/2}^{\pi/2}\frac{f^2(\theta)}{2}\cos\left(\frac{2\pi(x-y)}{\lambda}\sin\theta\right)d\theta\ . \tag{5}$$

Equation (5) shows that $R(x,y)$ is a symmetric function solely of the displacement $(x-y)$. In fact, it is a true autocorrelation function. The above expression essentially relates the source intensity $f^2(\theta)$ to the autocorrelation. A Fourier transform relationship can be developed as follows.

Let

$$s = (x-y)/\lambda \,. \tag{6}$$

Then the autocorrelation relationship becomes

$$R(s) = \int_{-\pi/2}^{\pi/2} \frac{f^2(\theta)}{2} \cos(2\pi s \sin\theta)\, d\theta \tag{7}$$

Put

$$t = \sin\theta \tag{8}$$

We then have

$$R(s) = \int_{-\infty}^{\infty} g(t) \cos(2\pi s t)\, dt \tag{9}$$

Where

$$g(t) = \begin{cases} \dfrac{f^2(\sin^{-1} t)}{2\sqrt{1-t^2}} & |t| \le 1 \\ 0 & \text{otherwise.} \end{cases} \tag{10}$$

Equation (9) indicates that the autocorrelation $R(s)$ and the derived field intensity function $g(t)$ form a Fourier transform pair. There is thus the possibility that, from an estimate of the autocorrelation, the extended object can be synthesized.

Simulations were performed with a discretized version of the problem by implementing the relationship in(7). Figure 6 shows an input object (essentially the squared magnitude of field strength) generated as a function of θ with 243 samples between $-\pi/2$ and $\pi/2$.

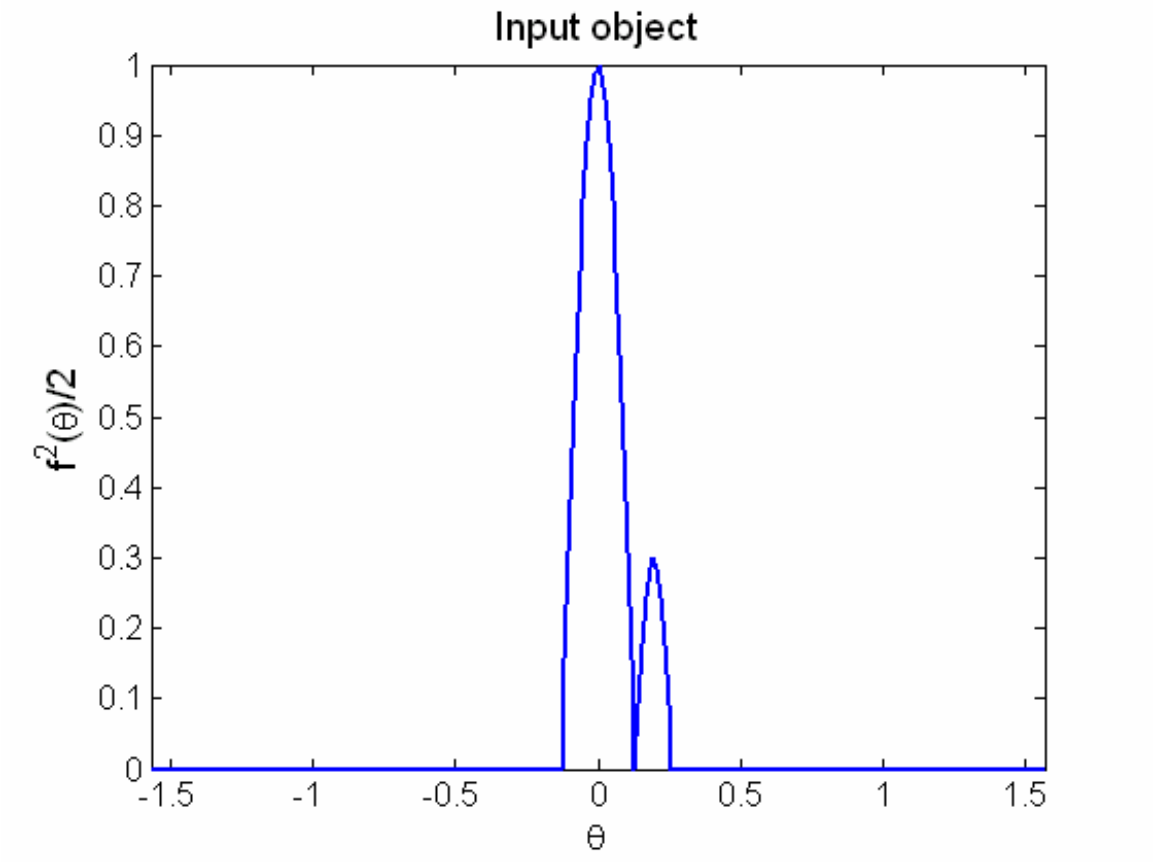

Figure 6. Input object.

Figure 7 shows 243 samples of the autocorrelation obtained from (7) for an array spacing of 0.2 wavelengths. The corresponding 243×243 matrix is singular with a rank of 64.

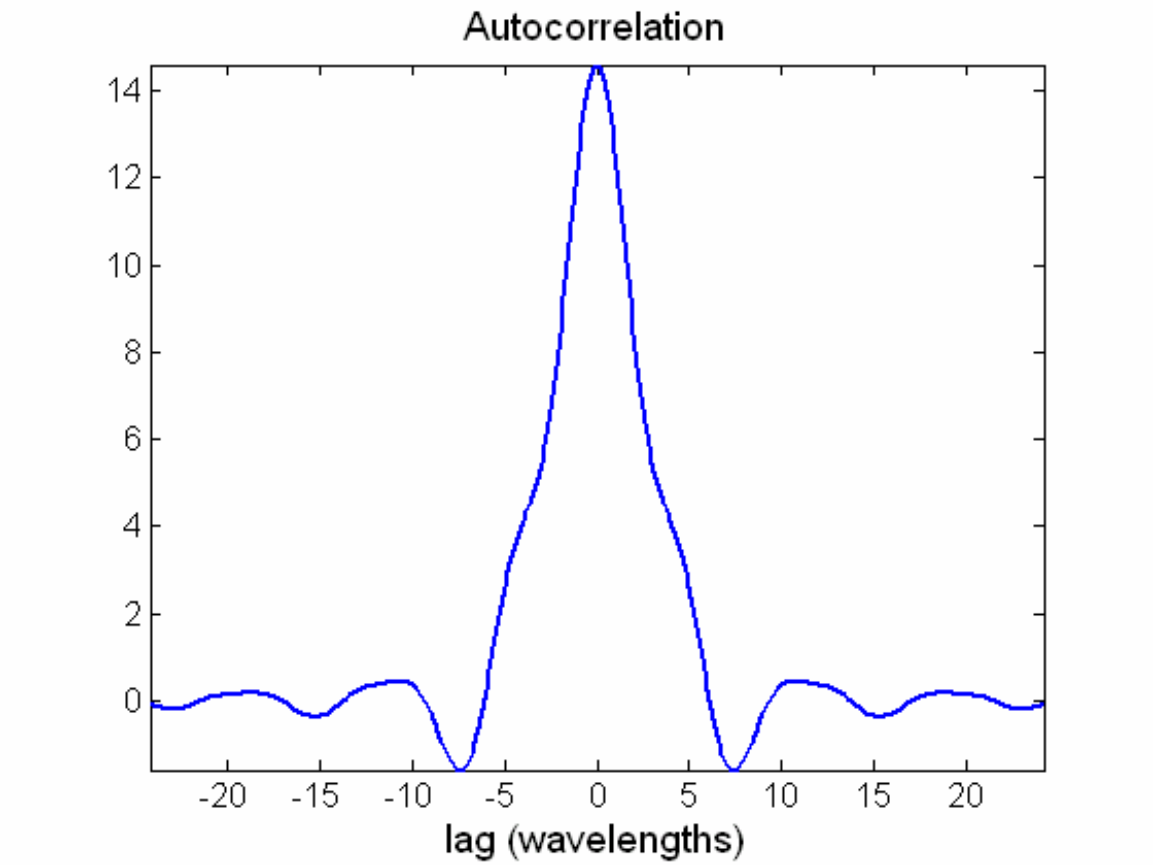

Figure 7. Autocorrelation

Figure 8 shows the reconstruction obtained from an unconstrained minimization as

$$\mathbf{f} = \arg\min_{\mathbf{x}} \left\| A\mathbf{x} - \mathbf{r} \right\|^2 \tag{11}$$

where A is the matrix transforming the object to the autocorrelation through the discretization of (7) and $\mathbf{r}$ is the recorded autocorrelation. In practice, the autocorrelation is not available and has to be estimated from data samples. The unconstrained reconstruction in Figure 8 is grossly different from the true object.

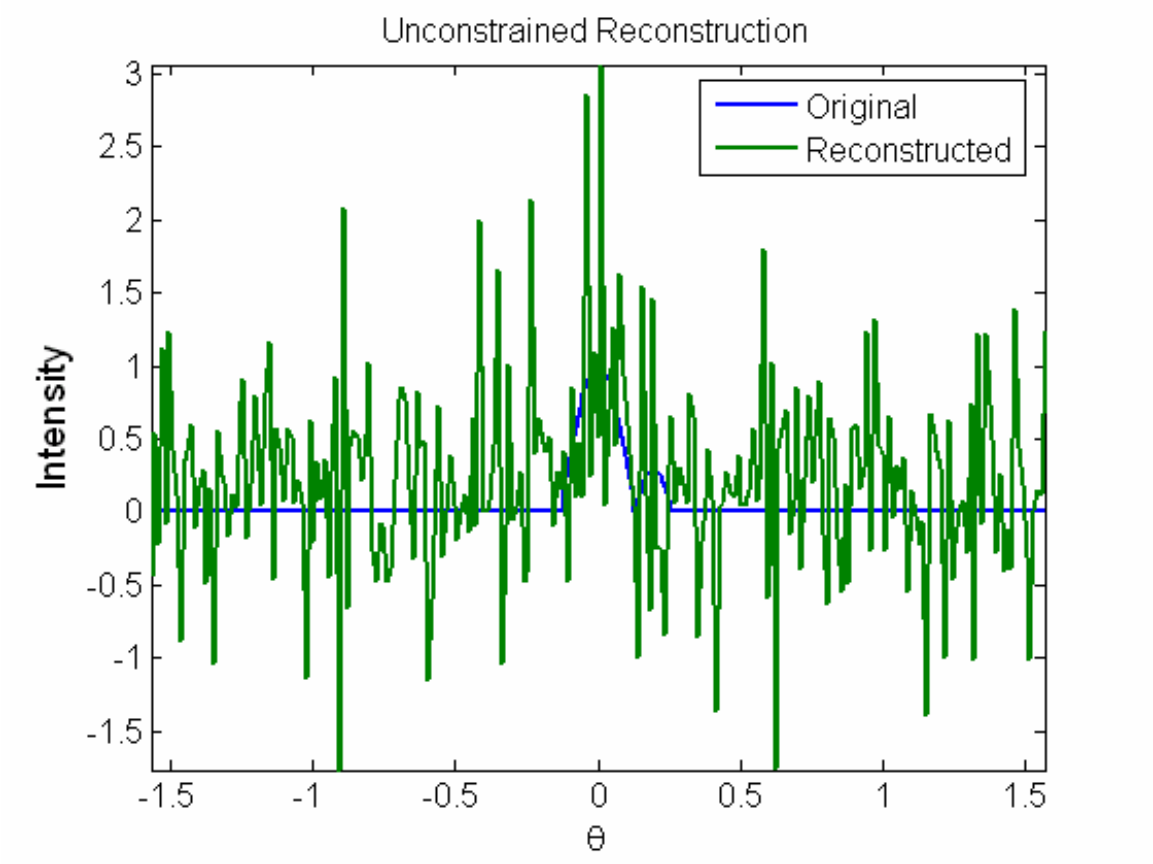

Figure 8. Result of unconstrained optimization

Imposing a positivity constraint on the solution yields the reconstruction shown in Figure 9.

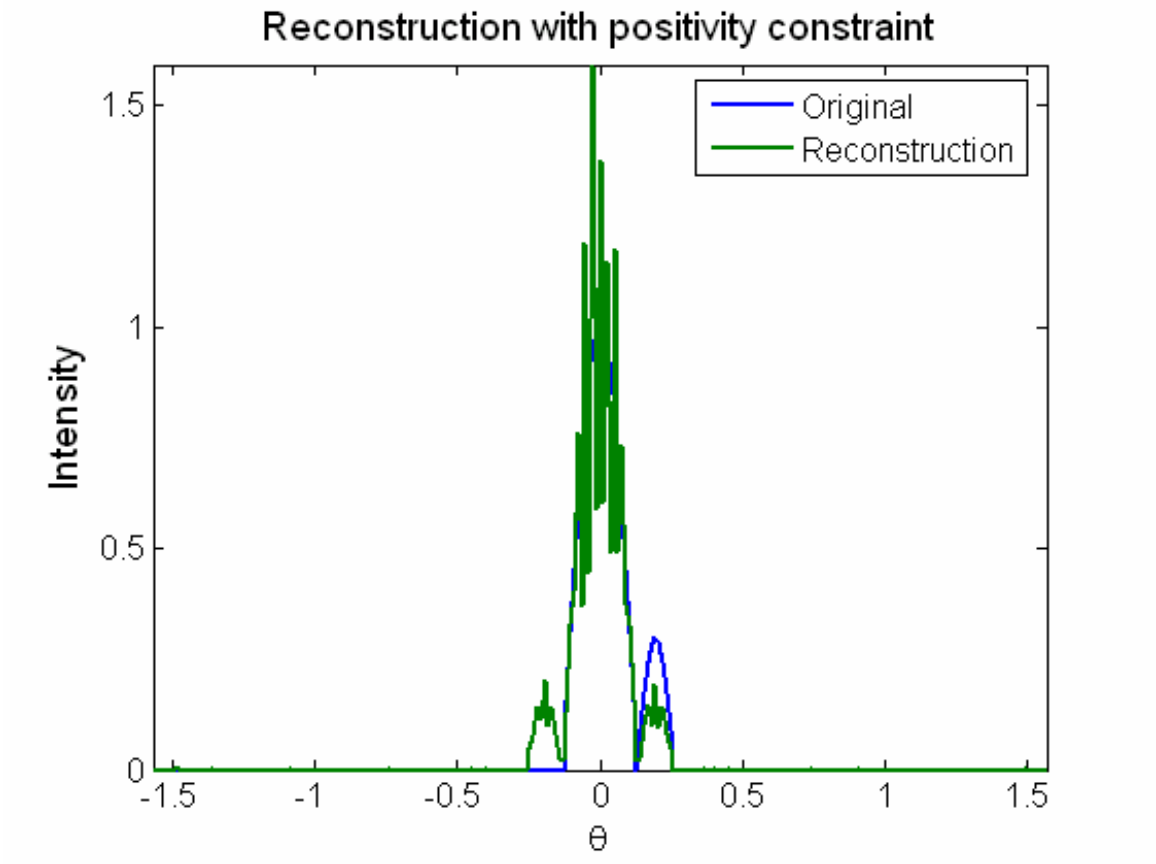

Figure 9. Result of applying positivity constraint only.

A noisy reconstruction of the taller component of the object seems to result from this constraint. Limiting the reconstruction boundary to the true limits results in the reconstruction of shown in Figure 10.

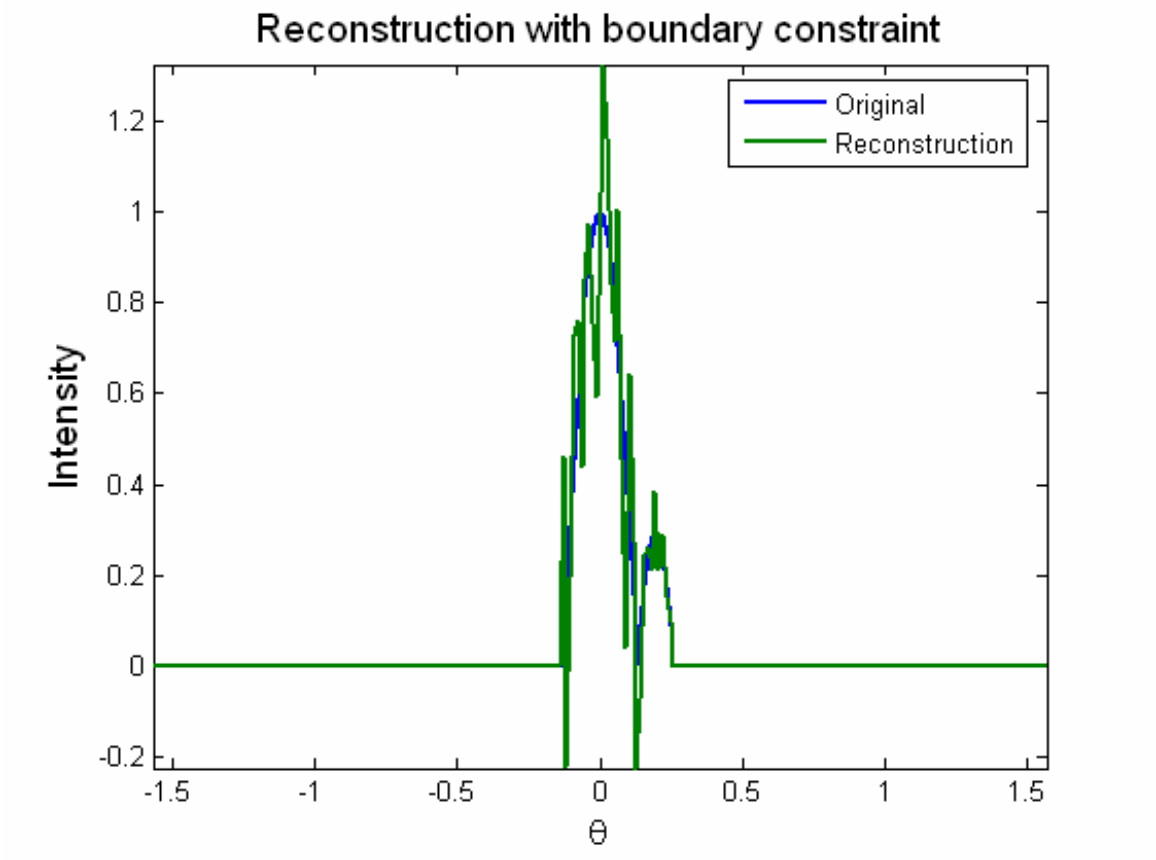

Figure 10. Result of applying boundary constraint only

The positivity constraint was not imposed and it is seen to be violated. Figure 11 shows a reconstruction with both the positivity and boundary constraints applied.

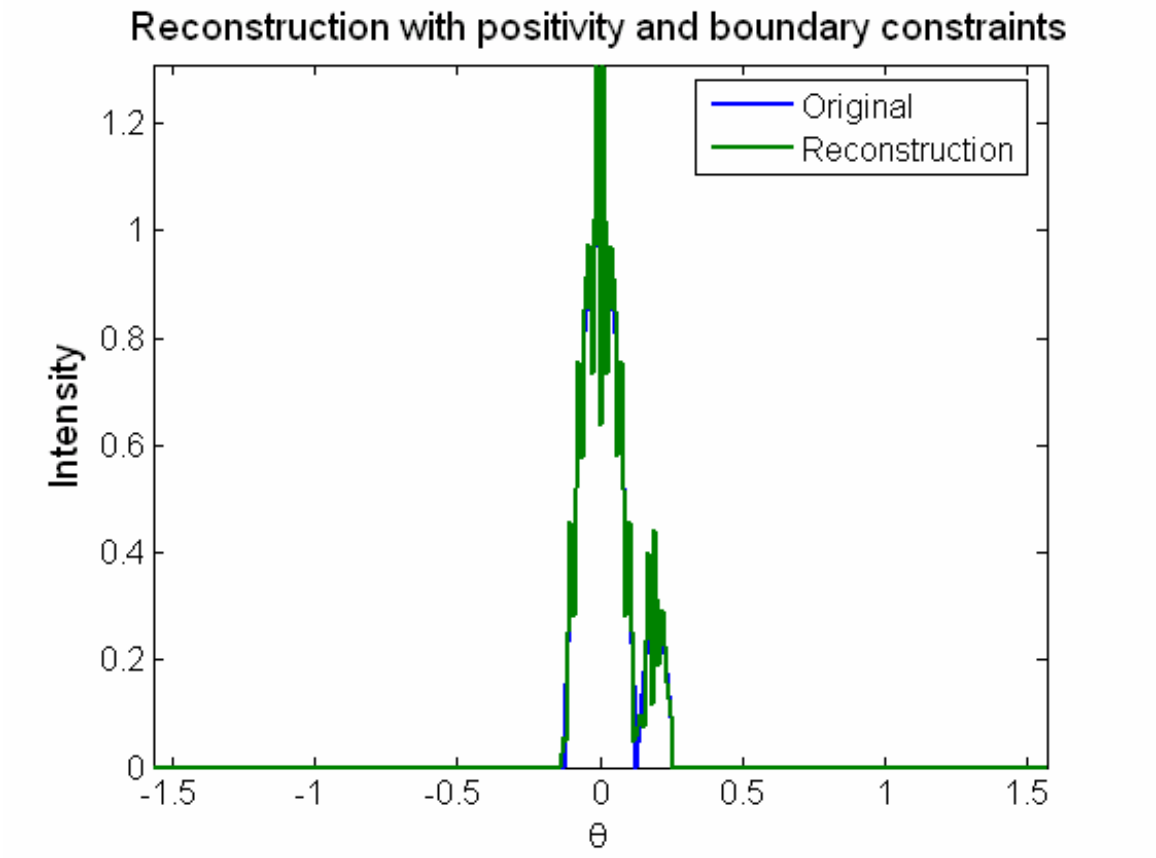

Figure 11. Both constraints applied

The result is obviously a much closer reconstruction to the original. Figures 12 and 13 show reconstructions at two different SNRs.

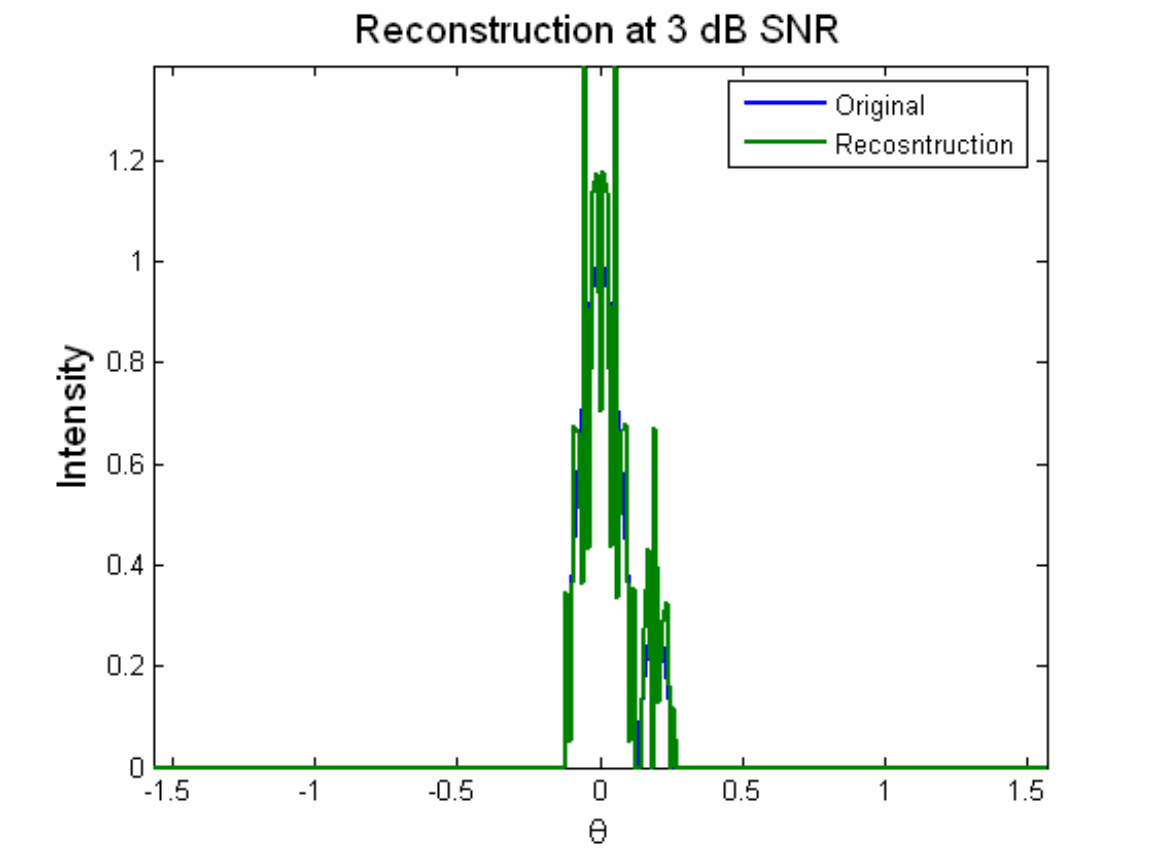

Figure 12. Reconstruction in noise. SNR=3 dB. Both constraints applied.

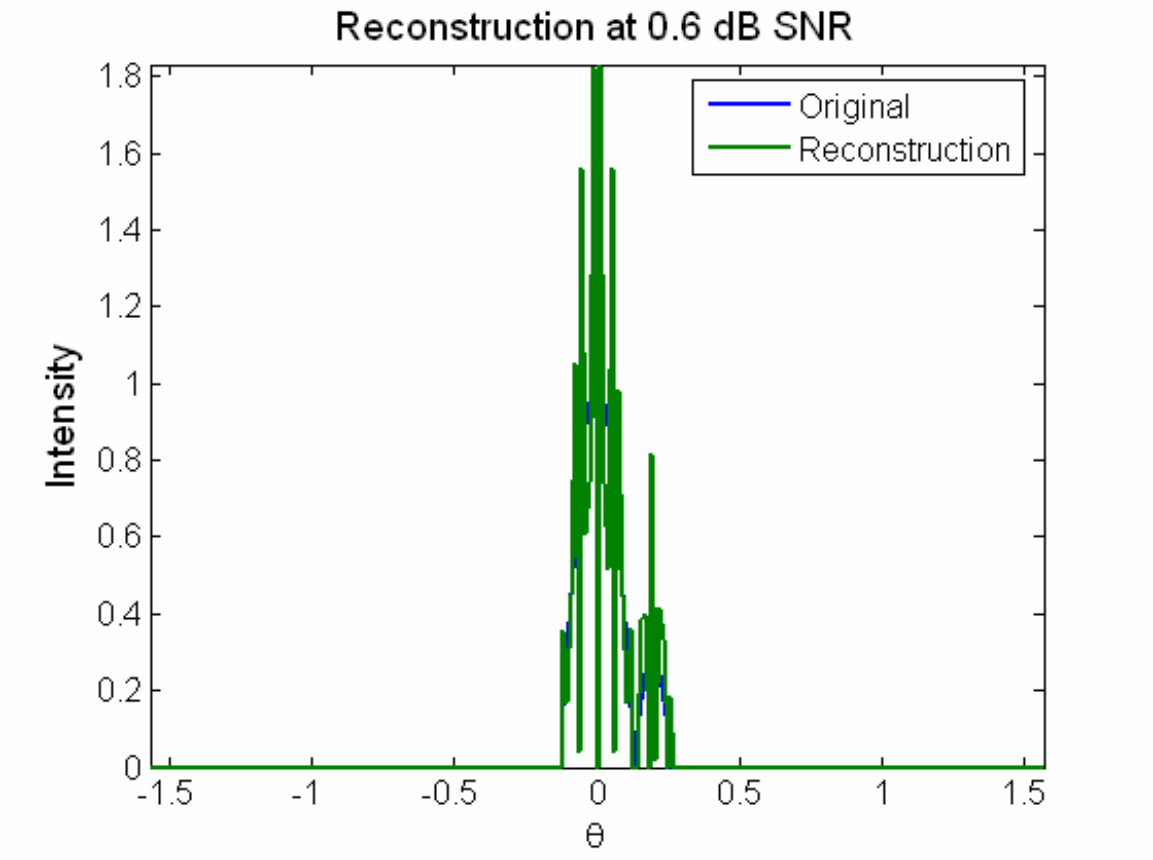

Figure 13. Reconstruction in noise. SNR=0.6 dB. Both constraints applied.

5.2 Near-Field Imaging

Terahertz imaging with antenna arrays has been proposed by Federici and colleagues [14]. They indicate that high resolution imaging necessarily involves working in the near-field. This opens the substantially unexplored subject of array signal processing for near-field data. This document contains preliminary results on the modeling and simulation using one-dimensional fields.

The field at a distance r from a point source field of strength E is

$$\frac{E}{r}\exp j\omega_0\left(t - r/c\right) \tag{12}$$

This may be rewritten as

$$\frac{E}{r}\exp j\left(\omega_0 t - 2\pi r/\lambda\right) \tag{13}$$

where λ is the wavelength. Thus the field phasor changes by an amount

$$\frac{E}{r}\exp\left(-j2\pi r/\lambda\right) \tag{14}$$

at a distance *r* from the source. Consider a line source and another line parallel to it at distance D wavelengths from it as shown in Figure 14.

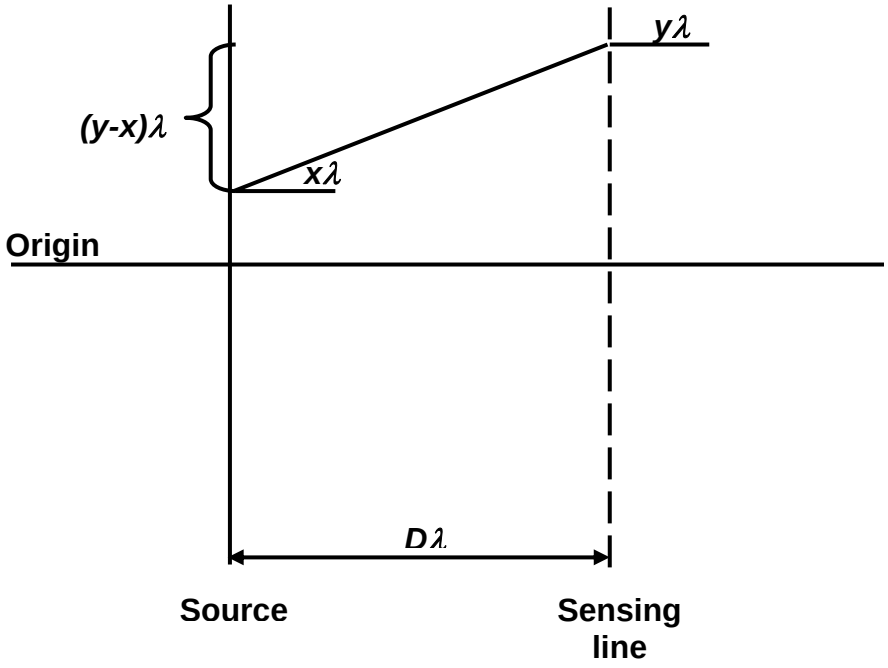

Figure 14. Source-sensing geometry

If $E(x)$ is the source field phasor at position $x\lambda$, the contribution from an elemental unit of length $d(x\lambda)$ in its neighborhood to the field at position $y\lambda$ on the sensing line is given (using Eq. (14)) by

$$\frac{E(x)}{\sqrt{D^2+(y-x)^2}}\exp\left(-j2\pi\sqrt{D^2+(y-x)^2}\right)dx \tag{15}$$

Thus, the sensed field $S(y)$ at $y\lambda$ is expressed as the convolution

$$S(y)=E(y)*h(y) \tag{16}$$

where * denotes the convolution operation, and

$$h(x) = A\frac{\exp\left[-j2\pi\sqrt{1+\left(\frac{x}{D}\right)^2}\right]}{\sqrt{1+\left(\frac{x}{D}\right)^2}} \text{ with}$$
$$A = \frac{\exp(-j2\pi D)}{D} \tag{17}$$

The term λ cancels out as a common factor. Equation (16) approximates to a Fourier transform relationship in the far field [15]. However, our interest is in working with this equation as is since we are considering the near-field. The function $h(x)$ may be regarded as an impulse response of a linear time-invariant system or as a Green's function for the particular geometry.

Suppose we have *N* observations at $s_1,\ldots,s_N$ at positions $y = \lambda x_1,\ldots,\lambda x_N$ respectively on the sensing line. We address the problem of reconstructing the source field $E(x)$ from these observations. From (16), we have

$$\begin{aligned} s_n &= E(x) * h(x)\big|_{x=x_n} \\ &= \int E(\nu)h(x_n-\nu)\,d\nu,\ n=1,\ldots,N. \end{aligned} \tag{18}$$

The problem is one of reconstructing $E(x)$ from the known function $h(x)$ and the values of s_n and x_n. Obviously, it is generally impossible to reconstruct a continuous function from a finite number of equations. One may find a least squares solution by finding $E(x)$ that minimizes

$$\sum_n \left| s_n - \int E(\nu)h(x_n-\nu)\,d\nu \right|^2 \tag{19}$$

This will mean finding a solution to the equation

$$\int E(\nu)\sum_n h(n-\nu)h^*(n-\mu)\,d\nu = \sum_n s_n h^*(n-\mu) \text{ for all } \mu \tag{20}$$

Variations of this equation appear in various sampling contexts [16]. An expression can be obtained in terms of the Fourier transform of $E(x)$. However, it is unwieldy and does not point to how one might solve (20). Furthermore, it should be clear that there are many

potential solutions. Further constraints need to be imposed to generate a unique solution. We develop the approach through simulation examples of a discretization of the problem. Correlative interferometry can be developed for the near field as well. Suppose we now model the source field at point $x\lambda$ as

$$E(x,t) = E(x)\exp j\omega_0 t = \left|E(x)\right|\exp j\left(\omega_0 t + \Phi_x\right) \tag{21}$$

where Φ_x is a random variable uniformly distributed between $-\pi$ and π. We assume further that this phase term is spatially uncorrelated, that is,

$$E\left\{\Phi_x \Phi_y\right\} = 0 \tag{22}$$

for $x \neq y$. Here $E\{\ \}$ is the expectation operator. Equation (22) corresponds to situation where we have a non-coherent source or illumination.

The spatial correlation of the sensed field is given by

$$\begin{aligned} &E\left\{S(x,t)S^*(y,t)\right\} \\ &= \frac{1}{D^2}\int_L \int_L \left|E(\lambda)\right|\left|E(\mu)\right| f(x-\lambda)\, f^*(y-\mu) \\ &\qquad \times E\left\{\exp j\left(\Phi_\lambda - \Phi_\mu\right)\right\} d\lambda\, d\mu \end{aligned} \tag{23}$$

where

$$f(x) = \frac{\exp\left(-j\pi\left(\frac{x}{D}\right)^2\right)}{1+\frac{1}{2}\left(\frac{x}{D}\right)^2} \tag{24}$$

It follows from (22) that

$$E\left\{\exp j\left(\Phi_\lambda - \Phi_\mu\right)\right\} = 0 \text{ for } \lambda \neq \mu. \tag{25}$$

Also, the right-hand side of (23) is not a function of *t*. Therefore, we have

$$\begin{aligned} R(x,y) &\equiv E\left\{S(x,t)S^*(y,t)\right\} \\ &= \frac{1}{D^2}\int_L \left|E(\lambda)\right|^2 f(x-\lambda)\, f^*(y-\lambda)\, d\lambda \\ &= \int_L \left|E(\lambda)\right|^2 g(x-\lambda, y-\lambda)\, d\lambda \end{aligned} \tag{26}$$

where $R(x,y)$ denotes the spatial correlation of the sensed field. Equation (26) shows that it is a linear transformation of the source intensity through the spatially varying kernel

$$g(x,y) \equiv \frac{f(x)\, f^{*}(y)}{D^2} \tag{27}$$

If $R(x,y)$ is available, then reconstructing the source intensity $|E(\lambda)|^2$ from (26) requires generating a solution to an integral equation. Since real-world measurements are from an array that samples on the sensing line, we turn our attention to the problem of reconstructing with such samples. Suppose we are given *N* spatial observations $s_1(t),\ldots,s_N(t)$ at positions $y = \lambda y_1,\ldots,\lambda y_N$ respectively on the sensing line. From (26), we have

$$R(y_m, y_n) = \int_L |E(\lambda)|^2 g(y_m - \lambda, y_n - \lambda)\, d\lambda \tag{28}$$

Solving for the intensity in (28), given the spatial correlation values between the sensors, amounts to reconstructing a continuous function from a finite number of discrete values, clearly an ill-posed problem. Further constraints are required to generate a unique solution.

We can discretize the problem further by approximating (28) in terms of samples of the source image as

$$R(y_m, y_n) = \sum_{k=1}^{M} |E(x_k)|^2\, g(y_m - x_k, y_n - x_k) \tag{29}$$

where *M* samples of the source image have been considered at $x_1, x_2,\ldots,x_M$ respectively. If $M = N^2$, one could try solving (29) with as many equations as unknowns. If $M < N^2$, that is, with more equations than unknowns, we can use a pseudo-inverse solution. However, the following issues need to be addressed:

1. Constraints may have to be imposed on the solution. At a minimum, a positivity constraint may be needed since we are reconstructing the source intensity.
2. In practice, we have access to the field measurements and not to the spatial correlation.

We therefore propose a constrained minimization approach using estimates of the correlation. Suppose $\hat{R}(y_m, y_n);\ \ m,n=1,\cdots,N$ are the estimates of the spatial correlation. We solve

$$\arg\min C(I_k) = \sum_{m=1}^{N}\sum_{n=1}^{N}\left|\hat{R}(y_m, y_n) - \sum_{k=1}^{M} I_k g(y_m - x_k, y_n - x_k)\right|^2 \tag{30}$$

subject to:

1. Positivity constraint on I_k.
2. Boundary constraint on I_k.

Here the I_k s are estimates of the source intensity at $x_1, x_2, \ldots, x_M$.

Simulations were performed assuming availability of true correlation values. Figure 15 shows an image whose cross-sectional profile is the one-dimensional object of interest.

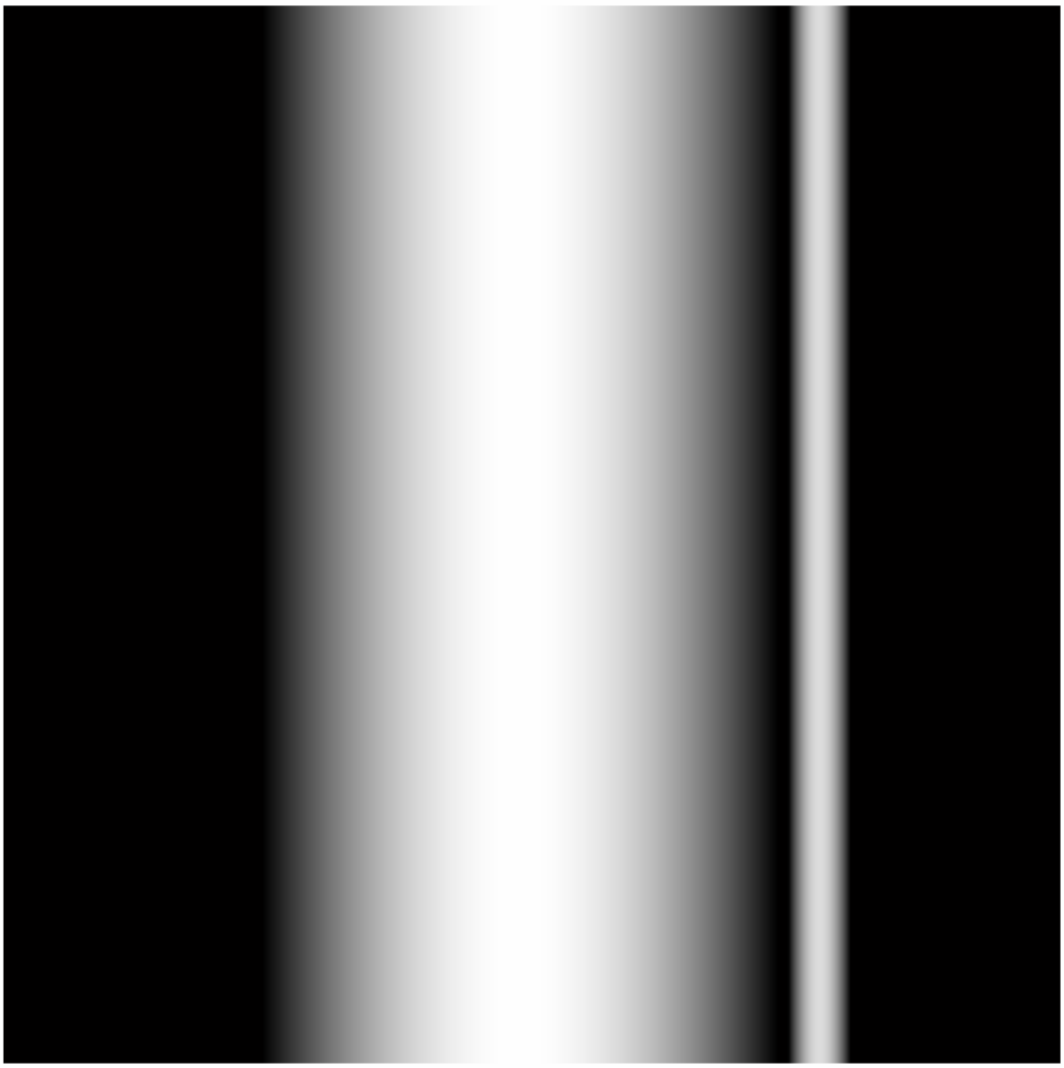

Figure 15. Input object

The horizontal axis consists of 41 samples taken over a distance of 400 wavelength units although the object itself is much smaller. The 41x41 matrix transforming the input field to the sensed field is singular. Figure 16 shows an unconstrained reconstruction while Figure 17 shows a reconstruction obtained with a positivity constraint and a support constraint which restricts the reconstruction to the support region of the input object. The use of such constraints is characteristic of various super-resolution techniques. Needless to say, the support constraint results in a reconstruction closer to the true field. However, the difference clearly shows that further constraints may be needed to generate a unique solution.

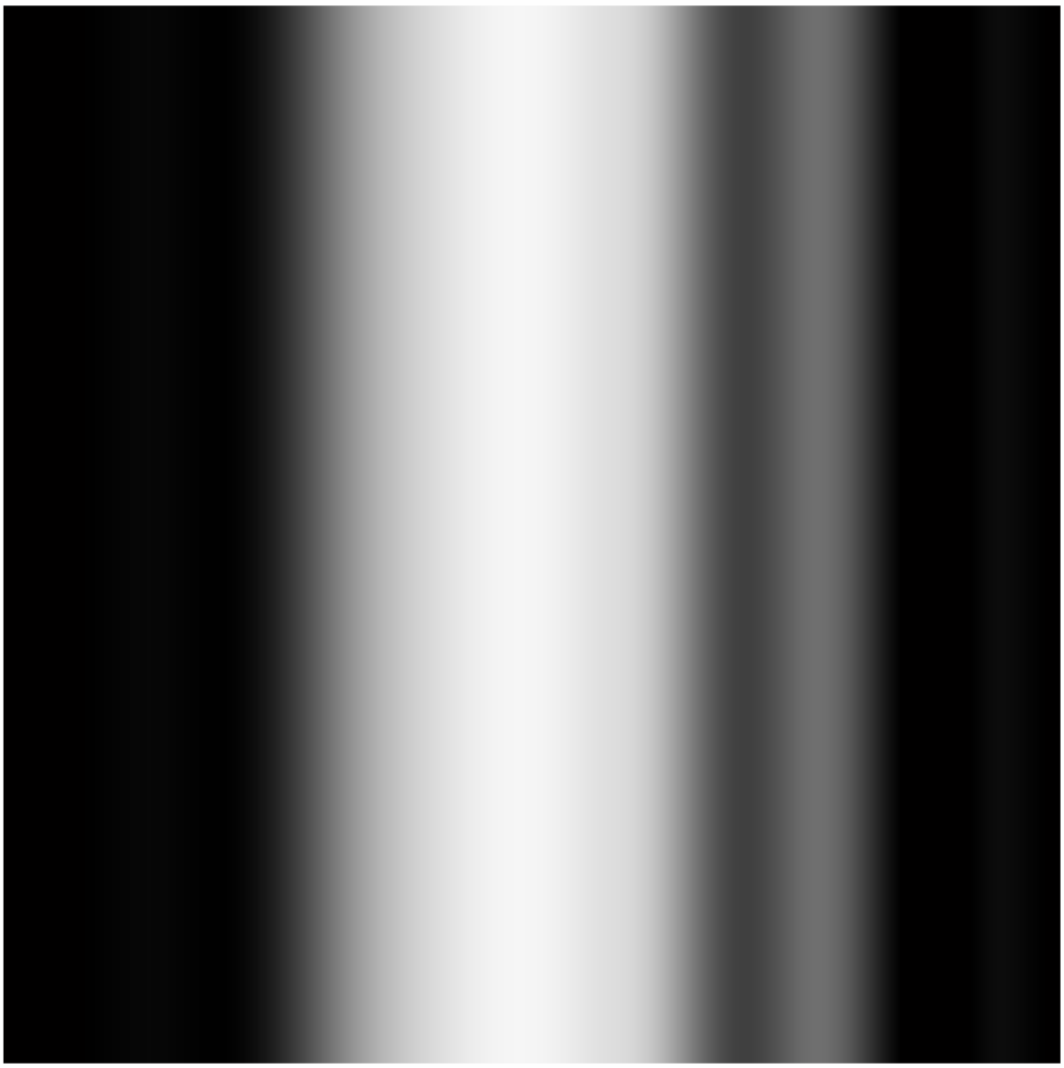

Figure 16. Unconstrained reconstruction

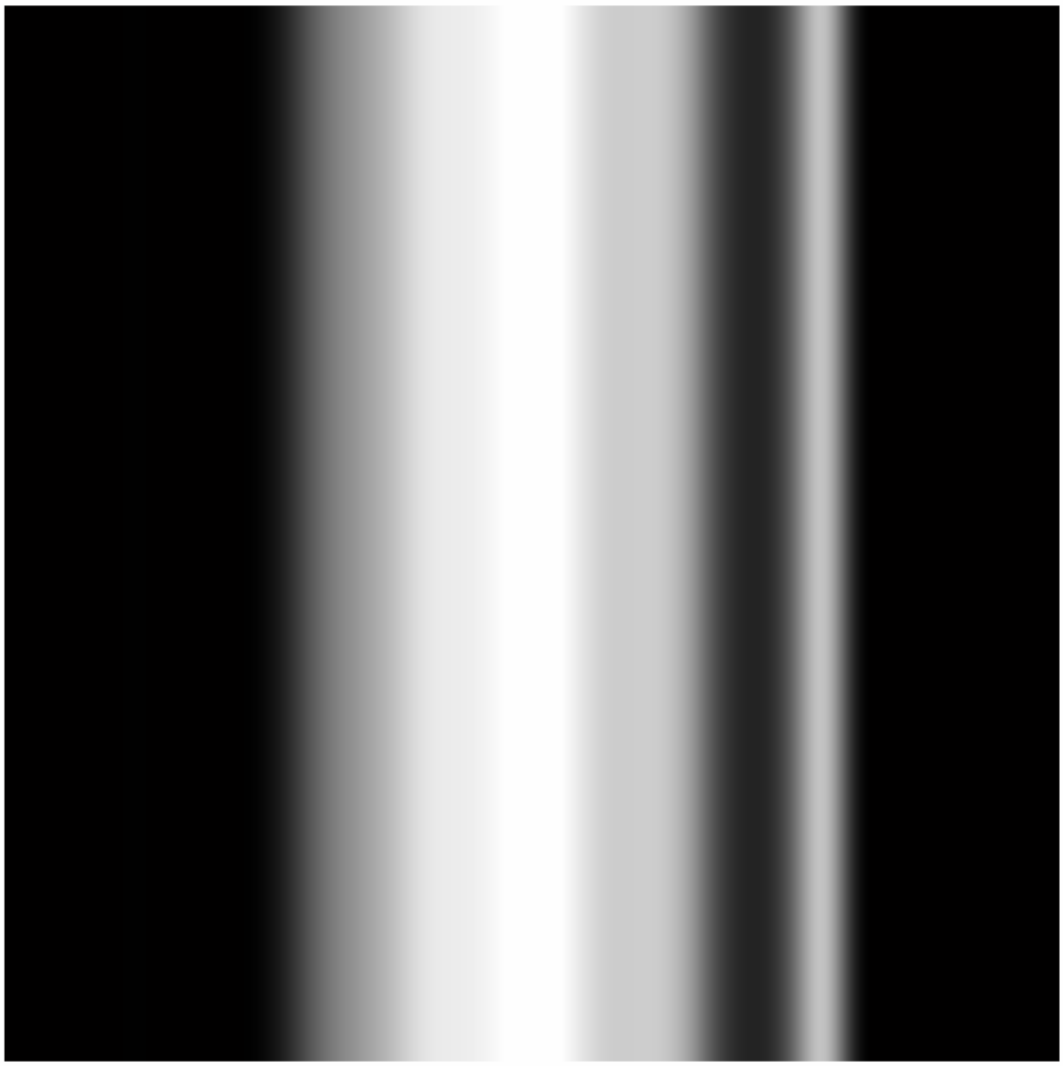

Figure 17. Reconstruction with positivity and boundary constraints.

6. Conclusions and Future Work

The assignment has identified Terahertz imaging for standoff detection of concealed objects as worthy of pursuit by AFRL/SNRT. The future success of THz imaging rests not only on progress in optoelectronic and electromagnetic generators and detectors but also on the development of signal processing algorithms. Our investigation has shown that interesting and important problems for THz image reconstruction from multisensor arrays can be formulated. Preliminary solutions have also been provided. To this date, two publications have resulted from this work Further investigation is necessary to test the performance of the algorithms and refine them for speed and robustness with respect to impairments such as noise, sensor positioning errors etc.

Some investigation was also conducted into tomographic reconstruction of complex fields in collaboration with 2nd Lt. Joshua Markow, AFRL/SNRT. The idea here is to take advantage of the fact that, unlike x-rays which offer only magnitude information, THz offers phase information. as well. While the magnitude contains attenuation information, the phase contains information about the refractive index. The investigation has revealed that phase reconstruction is very sensitive to noise and aliasing. Future work can investigate methods of mitigating the amount of phase errors.

A range of THz frequencies that is yet to be explored is in the neighborhood of 30 THz (wavelengths in the neighborhood of 10.6 micron or the carbon dioxide wavelength). As pointed out by Domenico Luisi, AFRL/SNRD, there is very little water vapor absorption at these wavelengths and the radiation can travel much larger distances than the commonly used range that falls under 3 THz. There is thus the possibility that detection can be accomplished at greater standoff distances. However, substantial spectroscopic work is needed in this area.

Investing in the development of new signal processing algorithms offers the greatest near term (3 to 5 year time frame) return is in interferometric tomographic reconstruction from antenna arrays. The key mathematical problems here are that of:

1. Relating field or intensity at source to antenna array measurements at a given wavelength.
2. Estimating source field or intensity from above relationship in the presence of impairments such as finite apertures, illumination issues and noise.

The interferometric approach relies on exploiting correlation and spatial diversity in the antennas located at different geographic locations. Several different scenarios for tomographic reconstruction in the order of increasing complexity are outlined below:

1. Far field passive reconstruction.
2. Near field passive image reconstruction.
3. Multistatic image construction with active illumination.

All of the scenarios above are worthy of investigation. The results of scenarios 1 and 2 are needed to carry out investigation of scenario 3. Passive reconstruction assumes continuous and uniform illumination. The reconstruction algorithms developed for passive scenarios can be embedded as components within the active multistatic image reconstruction algorithms.

7. References

[1] H.-M. Chen, S. Lee, R. M. Rao, M.-A. Slamani, and P. K. Varshney, "Imaging for concealed weapon detection: a tutorial overview of development in imaging sensors and processing," *IEEE Signal Processing Magazine. Special Issue on Surveillance Networks*, vol. 22, pp. 52-61, 2005.

[2] D. M. Mittleman, *Sensing with Terahertz Radiation*. New York, NY: Springer, 2003.

[3] J. F. Federici, R. Barat, D. Gary, and D. Zimdars, "THz standoff detection and imaging of explosives and weapons," *SPIE Photonics West*, 2005.

[4] P. H. Siegel, "Terahertz technology," *IEEE Transactions on Microwave Theory and Techniques*, vol. 50, pp. 910-28, 2002.

[5] W. Grill and O. Weis, "Excitation of coherent and incoherent Terahertz phonon pulse in quartz using infrared laser radiation," *Physical Review Letters*, vol. 35, pp. 588-91, 1975.

[6] W. Forkel, M. Welte, and W. Eisenmenger, "Evidence for 870-GHz phonon emission from superconducting Al tunnel diodes through resonant scattering by oxygen in silicon," *Physical Review Letters*, vol. 31, pp. 215-16, 1973.

[7] B. S. Patel and P. Swarup, "Rotational line overlap in CO2 laser transitions," *Journal of Physics D: Applied Physics*, vol. 6, pp. 1670-73, 1973.

[8] D. McDonald, "Josephson junctions as radiation detectors from millihertz to terahertz," *IEEE Journal of Quantum Electronics*, vol. 10, pp. 776-77, 1974.

[9] S. Mickan, D. Abbott, J. Munch, X.-C. Zhang, and T. van Doorn, "Analysis of system trade-offs for terahertz imaging," *Microelectronics Journal*, pp. 503-14, 1999.

[10] E. R. Mueller, "Terahertz radiation: applications and sources," *The Industrial Physicist Online*, vol. 9, pp. 29-31, 2003.

[11] D. M. Mittleman, R. H. Jacobsen, and M. C. Nuss, "T-ray imaging," *IEEE Journal of Selected topics in Quantum Electronics*, vol. 2, pp. 679-92, 1996.

[12] T. D. Dorney, W. W. Symes, and D. M. Mittleman, "Multistatic Reflection Imaging with Terahertz Pulses," *International Journal of High Speed Electronics and Systems*, vol. 13, pp. 677-99, 2003.

[13] J. F. Federici, D. Gary, R. Barat, and D. Zimdars, "Terahertz imaging using an interferometric array," in *Proceedings of the SPIE ---Terahertz for Military and Security Applications III*, vol. 5790, R. J. Hwu, D. L. Woolard, and M. J. Rosker, Eds.: SPIE, 2005, pp. 11-18.

[14] K. P. Walsh, B. Schulkin, D. Gary, J. F. Federici, and R. Barat, "Terahertz nearfield interferometric and synthetic aperture imaging," *Proceedings of SPIE -Terahertz for Military and Security Applications II*, vol. 5411, pp. 9-17, 2004.

[15] R. Bracewell, *The Fourier Transform and its Applications*. Boston: McGraw-Hill, 2000.

[16] R. M. Rao and A. S. Bopardikar, *Wavelet Transforms: Introduction to Theory and Application*. Reading, MA: Addison-Wesley Longman, 1998.

[17] R.M. Rao and B. Himed, "Constrained Optimal Interferometric Imaging of Extended Objects," *Applied Imagery and Pattern Recognition Workshop*, Washington DC, October, 2005.

[18] R.M Rao and B. Himed, "Correlative Interferometric Imaging of Extended Objects for Near Field Arrays," *First IEEE International Workshop on Computational Advances in Multi-Sensor Adaptive Processing*, Puerto Vallarta, Mexico, December 2005.

8. Annotated Bibliography of Recent Terahertz Imaging Publications

1. Wallace, V.P.; Fitzgerald, A.J.; Cole, B.C.; Pye, R.J.; Arnone, D.D., "**Biomedical applications of THz imaging**" Microwave Symposium Digest, 2004 IEEE MTT-S International , Volume: 3 , 6-11 June 2004, Pages: 1579 - 1581 Vol.3. (June 2004)

   Deals with optically driven terahertz systems and its biomedical applications such as detection of skin, tooth and breast cancer. The design and working of a THz imaging system capable of generating a usable frequency range of 0.1 to 3 THz is also explained. The paper also provides brief information about portable THz imaging systems.

2. Ogawa, Y.; Kawase, K.; Yawashita, M.; Inoue, H.; **"Non-destructive inspection techniques for illicit drugs using terahertz imaging"** Conference on Lasers and Electro-Optics, 2004. (CLEO)., Volume: 1 , May 17-19, 2004 Pages:88 – 90.

   Explains a novel basic technology for terahertz imaging; which allows detection and identification of drugs concealed in envelopes, by introducing the component spatial pattern analysis. The spatial distributions of the targets are obtained from terahertz multi spectral trans-illumination images, using absorption spectra measured with a tunable terahertz-wave source. The samples used were methamphetamine and MDMA, two of the most widely consumed illegal drugs in Japan, and aspirin as a reference. The three kinds of samples hidden in mail envelopes were clearly distinguished.

3. Markelz, A.G.; Chen, J.Y.; Knab, J.R.; Maeder, M.; **"Measuring protein flexibility with terahertz spectroscopy: basic research and applications"** Biophotonics/Optical Interconnects and VLSI Photonics/WBM Microcavities, 2004 Digest of the LEOS Summer Topical Meetings , Pages 28-30 June 2004.

   The experiment explained in this article uses terahertz time domain spectroscopy (TTDS) to **measure protein** dielectric response and investigate conformational vibrational modes. These modes known as conformational vibrational modes lie in the far infrared or terahertz frequency range. Thus this article uses terahertz time domain spectroscopy to measure the protein dielectric response and investigates conformational vibrational modes.

4. Ji Chen; Zekui Zhou; Xingnin Zhang; Tiehao Yu; **"Terahertz process tomography using in multiphase flow measurement"** Fifth World Congress on Intelligent Control and Automation, 2004. WCICA 2004., Volume: 4 , 15-19 June 2004 Pages:3727 - 3729 Vol.4.

   Focuses on terahertz process tomography technology that can be used in multiphase flow measurement. A prototype system of terahertz process tomography is described, and its structure, characteristics, arithmetic and feasibility are discussed. System performance and

industry application perspective are analyzed, specially compared with X-ray process tomography system.

5. Gregory, I.S.; Tribe, W.R.; Cole, B.E.; Baker, C.; Evans, M.J.; Bradley, I.V.; Linfield, E.H.; Davies, A.G.; Missous, M.; **"Phase sensitive continuous-wave THz imaging using diode lasers"** Electronics Letters , Volume: 40 , Issue: 2 , Pages:143 – 145, 22 Jan. 2004.

   Presents the preliminary results of a continuous-wave all-optoelectronic terahertz imaging system based on diode lasers. The coherent detection scheme is phase sensitive and operates at room temperature. The experiment results in low-cost, compact system having image capture rates comparable with those from state-of the-art pulsed THz systems. This is the first demonstration of such a compact, robust and low-cost system.

6. Ferguson, B.; Wang, S.; Xi, J.; Gray, D.; Abbott, D.; Zhang, X.-C.; **"Linearized inverse scattering for three dimensional terahertz imaging"** Conference on Lasers and Electro-Optics, 2003. CLEO '03., 1-6 June 2003.

   Uses two dimensional electro-optic sampling that allows a target's scattered terahertz field to be measured. By obtaining multiple projection images, reconstruction of three dimensional targets with millimeter resolution was performed. The reconstruction was performed using a frequency range of 0.2 THz, which provided the maximum SNR for the antenna source used. This reconstruction algorithm is only applicable to weakly scattering objects.

7. Buma, T.; Norris, T.B.; **"Time reversal 3-D imaging using single-cycle terahertz pulses"** Conference on Lasers and Electro-Optics, 2003. CLEO '03., 1-6 June 2003

   Explains demonstration of time reversal 3-D imaging using single-cycle terahertz pulses. The photoconductive transmitter and receiver are arranged in a reflection imaging configuration. The synthesized ring annular detection array can distinguish spatially separated image planes.

8. Zhong, H.; Xi, J.; Wang, S.; Zhang, X.-C.; **"T-ray tomography with a Fresnel lens"** Conference on Lasers and Electro-Optics, 2003. CLEO '03., 1-6 June 2003

   This article details in brief a demonstration of tomographic imaging with Fresnel lens, since Fresnel lens is lighter and compact than conventional THz optics. The article also reports about the possibilities of long range terahertz imaging with the same lens.

9. Wang, S.; Ferguson, B.; Zhong, H.; Zhang, X.-C.; **"Three-dimensional terahertz holography"** Conference on Lasers and Electro-Optics, 2003. CLEO '03., 1-6 June 2003 .

   This article demonstrates three-dimensional terahertz (THz) holography with the use of the windowed Fourier transformation. This paper explains that the coherent nature of THz time

domain spectroscopy allows measurement of the phase and amplitude of the THz wave for holographic imaging. Results of the demonstration have not been explained or shown in this article.

10. Evans-Pughe, C.; **"Sharper sight for surgeons"** IEE Review , Volume: 49 , Issue: 9 , Sept. 2003 Pages:40 – 43

This article states that terahertz radiation could become a new weapon in the fight against cancer due to its capacity to identify minute variations in soft tissue undetectable by other imaging methods. The radiation excites interactions between adjacent molecules and it's the secondary radiation produced by these molecular vibrations that provides the basis for cancer detection. The resulting spectral 'fingerprint' serves as an indicator of epithelial cancers (cancers in the area near the surface of various tissues such as skin, breast, prostate etc). This article describes Teraview's (University of Leeds) imaging system, its development and challenges to be overcome.

11. O'Hara, J.; Grischkowsky, D.; **"Coherent THz image processing and enhancement"** Conference on Lasers and Electro-Optics, 2003. CLEO '03., 1-6 June 2003 Pages:3 pp.

This report uses image processing to achieve spatial resolution enhancement for a coherent, synthetic, phased-array THz imaging system. The article states that these techniques eliminate higher order scattering processes, or clutter, and recover otherwise lost resolution in images of two abutting 397 /spl mu/m diameter spheres.

12. Zhang, X.-C.; "Recent progress of terahertz imaging technology" Conference on Optoelectronic and Microelectronic Materials and Devices, 11-13, Pages:1 – 6, Dec. 2002.

A perspective on state of art.

13. Wallace, V.P.; Arnone, D.A.; Woodward, R.M.; Pye RJ; "**Biomedical applications of terahertz pulse imaging**", [Engineering in Medicine and Biology, 2002. 24th Annual Conference and the Annual Fall Meeting of the Biomedical Engineering Society] EMBS/BMES Conference, 2002. Proceedings of the Second Joint , Volume: 3 , 23-26 Pages:2333 – 2334, Oct. 2002

Explains the biomedical opportunities for THz imaging since the technology behind optically-driven terahertz (THz) system is now well developed and commercial applications of this new technology are now beginning to emerge. The study describes the application of terahertz pulse imaging for imaging diseased tissue over a region of the electromagnetic spectrum, the THz region which has only recently opened up for this kind of investigation.

14. Wallace, V.P.; Cole, B.C.; Woodward, R.M.; Pye, R.J.; Arnone, D.A.; "Biomedical applications of terahertz technology" Lasers and Electro-Optics Society, 2002. LEOS 2002. The 15th Annual Meeting of the IEEE , Volume: 1 , Pages:308 – 309, 10-14 Nov. 2002 .
Similar to 13.

15. Herrmann, M.; Tani, M.; Watanabe, M.; Sakai, K.; **"Terahertz imaging of objects in powders"** Optoelectronics, IEE Proceedings- , Volume: 149 , Issue: 3 , Pages:116 – 120, June 2002,.
The use of terahertz radiation for-detecting and imaging objects hidden in powders is demonstrated in this paper. A simple method for distinguishing between objects of different materials even if their thickness is unknown is explained in this report. The potential of THz radiation for measuring the local density profile of powders is also demonstrated.

16. Ferguson, B.; Wang, S.H.; Abbott, D.; Zhang, X.-C.; **"T-ray tomographic imaging"** IEEE Tenth International Conference on Terahertz Electronics Proceedings, 2002., 9-10 Sept. 2002.
Reports about three THz wave tomographic imaging modalities: T-ray Computer Tomography (T-ray CT), T-ray Diffractive Tomography (T-ray DT) and tomographic imaging with Fresnel lens. T-ray CT provides 3D images and reveals information about the target for functional imaging. T-ray DT achieves sub-mm spatial resolution and binary lens leads to novel imaging modalities with broad band T ray pulses.

17. Zhang, X.-C.; "**Tomographic imaging with terahertz pulses"** Lasers and Electro-Optics Society, 2002. LEOS 2002. The 15th Annual Meeting of the IEEE Volume: 2, Pages: 528 – 529, 10-14 Nov. 2002.
Explains the advantages and the procedure involved in using Fresnel lens for tomographic imaging with THz radiation. The linearly frequency-dependent focal length of a Fresnel lens allows tomographic imaging of a target using multiple frequencies. Objects at various locations along the beam propagation path are uniquely imaged on the same imaging plane using a Fresnel lens with different frequencies of the imaging beam. This procedure allows the reconstruction of an object's tomographic contrast image by assembling the frequency-dependent images, and provides a new tomographic imaging modality.

18. Chamberlain, J.M.; Zinovev, N.N.; Fitzgerald, A.J.; Berry, E.; Walker, G.C.; Handley, J.W.; Smith, M.A.; Miles, R.E.; **"What constitutes a useful and meaningful terahertz image?"** IEEE Tenth International Conference on Terahertz Electronics Proceedings, 2002. Pages: 81 – 84, 9-10 Sept. 2002.

Attempts to answer the question how are the THz images best processed, analyzed, presented, classified ad interpreted with a clinical setting? Computer vision and data compression techniques are also discussed in the process. It concludes that compounded images, involving pulse broadening as an image parameter, are highly promising routes to visualization.

19. Zinov'ev, N.N.; Fitzgerald, A.F.; Strafford, S.M.; Wood, D.J.; Carmichael, F.A.; Miles, R.E.; Smith, M.A.; Chamberlain, J.M.; **"Identification of tooth decay using terahertz imaging and spectroscopy"** Infrared and Millimeter Waves, 2002. Conference Digest. Twenty Seventh International Conference on , 22-26 Sept. 2002 Pages:13 – 14 (September 2002).
The terahertz (THz) frequency spectroscopic imaging studies of teeth are reported. The aim of the experiment was to establish the characteristic properties of the enamel and dentine at these high frequencies. Changes to the THz characteristics as a result of various types of tooth decay are reported showing the potential of this technique for dental diagnosis.

20. Herrmann, M.; Tani, M.; Sakai, K.; Watanabe, M.; **"Towards multi-channel time-domain terahertz imaging with photoconductive antennas"** International Topical Meeting on Microwave Photonics, 2002., Pages:317 – 320, 5-8 Nov. 2002
Explains the working and results of a small and cheap, yet efficient electronic circuit for reading out THz signals from photoconductive antennas. An 8-channel version of this circuit has been used for THz imaging by simultaneously recording sets of 8 time-domain THz waveforms with an array of 8 photoconductive antennas.

21. Loffler, T.; Bauer, T.; Siebert, K.J.; Roskos, H.G.; Fitzgerald, A.; Czasch, S.; **"Investigation of tumor recognition by Terahertz dark-field imaging"** Lasers and Summaries of Papers Presented at the Electro-Optics, 2002. CLEO '02. Technical Digest. 19-24 May 2002 .
Demonstrates that the THz dark-field imaging, which allows enhancing of imaging contrast especially at tissue boundaries, holds for the clinical distinction between beginning and malignant tumors as this is usually based on the differences in the structure of the tumor boundary. This article states that dark-field imaging deals with contrast enhancement by the detection of that part of the radiation which is deflected out of the beam-propagation direction by either diffraction or scattering in the sample, and requires blocking of the ballistic part of the radiation.

22. Mittleman, D.M.; **"T-ray imaging: new possibilities in the far infrared"** Microwave Symposium Digest, 2002 IEEE MTT-S International , Volume: 3 , Pages:1575 – 1578, 2-7 June 2002

Describes one technique in terahertz imaging, which permits time-of-flight imaging with depth resolution well below the Rayleigh limit. These include implementations in reflection geometry, where the short duration of the THz pulses permits three-dimensional image reconstruction using time-of-flight techniques. The paper also discusses a new imaging technique involving interferometry, which can be used to resolve two reflecting surfaces which are separated by much less than the coherence length of the radiation.

23. Foulds, A.P.; Chamberlain, J.M.; Berry, E.; **"Terahertz imaging of wound healing"** High Frequency Postgraduate Student Colloquium, 2002.7th IEEE , 8-9 Sept. 2002 .
Explains an experimental system which was being built to produce images in the little used frequency range of 0.1-3 THz of the electromagnetic system. A system is described, based on a femtosecond laser using optical rectification to generate and electro-optic sampling to detect the terahertz radiation. Different types of THz images are introduced, and the application of THz imaging to wound healing is discussed.

24. Schildknecht, C.; Kleine-Ostmann, T.; Knobloch, P.; Rehberg, E.; Koch, M.; **"Numerical image enhancement for THz time-domain spectroscopy"** IEEE Tenth International Conference on Terahertz Electronics Proceedings, 2002., Pages:157 – 160, 9-10 Sept. 2002.
Explains the application of numerical image enhancement methods to THz time-domain spectroscopy images in order to improve the quality of experimental data suffering from low resolution and finite focus diameter aperture effects. As an example, the level of detail in a biomedical image of a histopathological sample is shown to increase significantly. The article presents the Jansson-Van-Cittert algorithm as a possible approach to numerical image enhancement of THz time domain spectroscopic images. Its states that numerical image processing has more applications in THz time domain spectroscopy than image enhancement. It also states that digital filtering can be used to calculate the derivative of the image profile in order to reveal and recognize edges enabling applications in THz packaging inspection.

25. Schmidt, L.-P.; Biber, S.; Rehm, G.; Huber, K.; "THz measurement technologies and applications" 14th International Conference on Microwaves, Radar and Wireless Communications, 2002. MIKON-2002., Volume: 2 , Pages:581 – 587, 20-22 May 2002.
Looks at THz detectors.

26. Herrmann, M.; Tani, M.; Sakai, K.; Watanabe, M.; **"Multi-channel signal recording with photoconductive antennas for THz imaging"** IEEE Tenth International Conference on Terahertz Electronics Proceedings, 2002., 9-10 Sept. 2002 Pages:28 – 31

Similar to [20]. Explains the working and results of a small and cheap, yet efficient electronic circuit for reading out THz signals from photoconductive antennas. An 8-channel version of this circuit has been used for THz imaging by simultaneously recording sets of 8 time-domain THz waveforms with an array of 8 photoconductive antennas.

27. Shaohong Wang; Ferguson, B.; Mannella, C.; Abbott, D.; Zhang, X.-C.; **"Powder detection using THz imaging"** Summaries of Papers Presented at the Quantum Electronics and Laser Science Conference, 2002. QELS '02. Technical Digest., 19-24 May 2002

Contains a brief description of the possibilities of using terahertz waves in detecting harmful substances such as explosives, illicit drugs and bioterrorism substances such as the Anthrax causing bacterium Bacillus anthracic. This article states that the nondestructive scanning of mail envelopes and packages by a chirped probe beam THz imaging system is a topic of current research interest.

28. Kleine-Ostmann, T.; Knobloch, P.; Koch, M.; Hoffmann, S.; Hofmann, M.; Hein, G.; Pierz, K.; **"Compact and cost-effective continuous wave THz imaging system"** Summaries of Papers Presented at the Lasers and Electro-Optics, 2002. CLEO '02. Technical Digest., Pages:405 – 406, 19-24 May 2002.

THz radiation is generated via photo mixing in a LT-GaAs dipole antenna. Research shows that during the last years THz technology has been developed to a stage where first commercial systems are available. Yet, the THz imaging systems developed so far all work in the time-domain using THz pulses. Hence, they rely on expensive and bulky femtosecond lasers as a key component. Therefore this article details a terahertz imaging setup that can generate frequencies from 0.2 to 0.5 THz.

29. Siebert, K.J.; Quast, H.; Leonhardt, R.; Loffler, T.; Thomson, M.; Bauer, T.; Roskos, H.G.; Czasch, S.; **"All-optoelectronic CW THz-imaging"** Summaries of Papers Presented at the Lasers and Electro-Optics, 2002. CLEO '02. Technical Digest., Pages:635 – 636, 19-24 May 2002 .

Demonstrates CW THz imaging with complex sample and compares the results with images taken with a state-of-the-art pulsed system based on an Ti:sapphire amplifier laser operating at 1-kHz repetition rate.

30. T. D. Dorney, W. W. Symes, R. G. Baraniuk, and D. M. Mittleman, "Terahertz multistatic reflection imaging," Journal of the Optical Society of America A, 19, 2002..

Applies seismic migration type techniques to image conducting objects in dielectrics.

31. Shen, Y.C.; Upadhya, P.; Davies, A.G.; Linfield, E.H.; **"Light-induced difference Terahertz spectroscopy and its biomedical applications"** Terahertz Electronics Proceedings, 2002. IEEE Tenth International Conference on , Pages:161 – 164, 9-10 Sept. 2002.

Uses laser-induced difference THz spectroscopy to investigate three samples with different lifetimes. The spectroscopy system is based on a 10 nJ titanium sapphire laser with a pulse duration of 12 fs and a centre wavelength of 790 nm. A lifetime of about 50 ps has been determined for the SI-GaAs sample, whereas the lifetime of the HR-Si samples was found to be much larger than the time interval between two successive laser pulses (12 ns). As a result, the differential THz signal is about twenty times larger than that for SI-GaAs. This article also observed that the THz pulse arrives at the detector 100 fs earlier when it transmitted through an optically excited HR-Si wafer.

32. De Lucia, F.C.; **"THz spectroscopy - techniques and applications"** Microwave Symposium Digest, 2002 IEEE MTT-S International, Volume: 3, Pages: 1579 – 1582, 2-7 June 2002.

Reviews established techniques and discuss new approaches in THz spectroscopy. Spectroscopy and elated applications have accounted for a large proportion of the work in the THz spectral region. These have included laboratory studies of the radiative and collisional properties of molecules, ions, and radicals, as well as field applications such as atmospheric remote sensing and molecular radio astronomy.

33. Kadlec, R.; Nemec, H.; Kuzel, P.; **"Frequency-domain approach to evaluation of data obtained in optical pump-terahertz probe experiments"** Twenty Seventh International Conference on Infrared and Millimeter Waves, 2002. Conference Digest. , Pages:23 – 24 22-26 Sept. 2002.

Describes the increasing effort to develop optical pump-terahertz probe (OPTP) experiments as a tool for studying transient processes following excitation by an optical pulse, e.g. in semiconductors, superconductors. A method is necessary to find the unknown non-equilibrium part of the response function so the authors of this article have developed a general frequency domain theory which can serve as a guide for performing the experiment.

34. Chen, Q., Zhang, X.-C., "**Semiconductor dynamic aperture for near-field terahertz wave imaging**", Selected Topics in Quantum Electronics, IEEE Journal of Quantum Electronics, Volume: 7 , Issue: 4 , pages 608 – 614, July-Sept. 2001.

Describes and discusses near-field terahertz wave imaging with a dynamic aperture created on a semiconductor wafer. The spatial resolution of a near-field terahertz wave imaging system with a dynamic aperture created on a GaAs wafer is determined by the diameter of the gating-

beam-induced thin photo carrier layer. With a dynamic aperture created on a GaAs wafer, the experiment achieved a sub wavelength spatial resolution of ~λ/10. In addition, near-field terahertz wave imaging with a dynamic aperture overcomes the limitations in the reported methods of near-field terahertz wave imaging. Various terahertz images are presented to show the possible applications.

35. Johnson, J.L.; Dorney, T.D.; Mittleman, D.M.; **"Interferometric imaging with terahertz pulses"** IEEE Journal of Selected Topics in Quantum Electronics, , Volume: 7 Issue: 4 , July-Sept. 2001. Pages:592 – 599, July 2001.

Demonstrates a new reflection imaging technique using single-cycle pulses, in which the sample to be imaged is placed at the focus of a lens in one arm of a Michelson interferometer. The detected signal is the superposition of the pulses from the two arms of the interferometer, one with a sample and one with a reference mirror leading to a strong cancellation of the measured waveform and a nearly background-free imaging method. This report details the demonstration of the technique using terahertz time-domain spectroscopy and show that the destructive interference provides enhanced sensitivity to features in the sample that are much thinner than the coherence length of the radiation.

36. Mitrofanov, O.; Lee, M.; Hsu, J.W.P.; Brener, I.; Harel, R.; Federici, J.F.; Wynn, J.D.; Pfeiffer, L.N.; West, K.W.; "**Collection-mode near-field imaging with 0.5-THz pulses**" IEEE Journal of Selected Topics in Quantum Electronics, , Volume: 7 , Issue: 4 , Pages:600 – 607, July-Sept. 2001

Since high spatial resolution imaging with terahertz pulses is implemented with a novel collection-mode near-field probe. The spatial resolution capabilities of the system are in the range of few micrometers. This paper demonstrates resolution of 7 m using 0.5-THz pulses and discusses performance of the collection-mode near-field probes and image properties.

37. Mitrofanov, O.; Harel, R.; Lee, M.; Pfeiffer, L.N.; West, K.W.; Wynn, J.D.; Federici, J.; **"THz transmission near-field imaging with very high spatial resolution"** Summaries of papers presented at the Conference on Lasers and Electro-Optics, 2001. CLEO '01. Technical Digest., Pages:515 – 516, 6-11 May 2001

Discusses the attenuation of single-cycle THz pulses for various aperture sizes (10-50 μm). The near-field probe with the 10 gm aperture provides spatial resolution of ~10 μm at the wavelength range from 120 to 1500 μm. Also according to the explanation in this paper, it is the highest resolution achieved with THz pulses in this spectral range. Near-field images can be constructed with signal to noise ratio of ~50.

38. Cheville, R.A.; Grischkowsky, D.; **"Reflective geometry THz imaging"** O'Hara Summaries of papers presented at the Conference on Lasers and Electro-Optics, 2001. CLEO '01. Technical Digest., Pages:439 – 440, 6-11 May 2001.

Describes a method using reflection geometry where the THz beam illuminates the target and its reflections are collected and measured. Unlike others, this method allows the measurement of non-uniform, opaque objects. This method generated useful spectra bounded between 0.2 THz and 2 THz that was used in the measurement of opaque objects.

39. Kleine-Ostmann, T.; Knobloch, P.; Koch, M.; Hoffmann, S.; Breede, M.; Hofmann, M.; Hein, G.; Pierz, K.; Sperling, M.; Donhuijsen, K.; **"Continuous-wave THz imaging"** Electronics Letters , Volume: 37 , Issue: 24 , Pages:1461 – 1463., 22 Nov. 2001

The first THz imaging spectrometer based on continuous-wave THz radiation is presented in this article. This article states that the new setup is less expensive than conventional time-domain imaging systems that comprise femtosecond lasers. The system uses a two-color external-cavity laser diode. Therefore it is more compact as compared to systems based on optically pumped solid-state lasers. As an example investigation of a human liver with metastasis is conducted and detailed in this report.

40. C. Benzant: "Application of THz pulses in semiconductor relaxation and Biomedical Imaging Studies" PhD thesis, (2000) (University of Nottingham, United Kingdom)

41. S.Mickan, D. Abbott, J. Munch, X. –C. Zhang and T. van Doorn: "Analysis of system trade-offs for terahertz imaging" Microelectronics Journal 31, pages 503 – 514, 2000.

Discusses potential of MEMS technology for terahertz imaging.

42. Dorney, T.D.; Baraniuk, R.G.; Mittleman, D.M.; "**Spectroscopic imaging using terahertz time-domain signals**", Image Analysis and Interpretation, 2000. Proceedings. 4th IEEE Southwest Symposium , 2-4 Pages:151 – 155, April 2000.

Describes a robust algorithm for extracting both the thickness and the complex index of refraction of an unknown sample. There exists a range of modalities due to broad bandwidth, sub-picosecond duration and phase sensitive detection of the THz pulses in imaging systems based on terahertz time domain spectroscopy. And since due to these modalities, both the absorption and the phase delay of a transmitted THz pulse vary exponentially with the sample's thickness.

43. Jiang, Z.; Zhang, X.-C.; **"Improvement of THz imaging"** Conference on Lasers and Electro-Optics, 2000. (CLEO 2000)., Pages:464 – 465, 7-12 May 2000

Adopts the principle of the lock-in detection in a CCD THz imaging system thereby greatly improving the SNR because in CCD based THz imaging system the lock-in amplifier that suppresses the noise greatly can not be used with the CCD imager, therefore the CCD-based THz imaging system suffers from low signal-to-noise ratio (SNR). As an example, the 2D distribution of the relatively weak THz pulses generated by an optical rectification emitter is measured.

44. Johnson, J.L.; Dorney, T.; Mittleman, D.;"Background-free THz imaging using interferometric tomography" Conference on Lasers and Electro-Optics, 2000. (CLEO 2000), Pages:526 – 527, 7-12 May 2000.

45. Reiten, M.T.; McGowan, R.W.; Grischkowsky, D.R.; Cheville, R.A.; **"THz imaging, ranging, and applications"** Conference on Lasers and Electro-Optics, 2000, Pages:525 – 526, 7-12 May 2000.

Explains in brief the generation of THz pulses using micron scale dipole antennas and the applications of the generated pulses. It explains that the combination of ultra short optical pulses with micron scale dipole antennas permits generation of single cycle electromagnetic radiation. The pulses generate ultra wide band widths, which can cover two decades of frequency. This article states that the near-impulse, ultra wide band excitation has advantages for various ranging measurements such as measurement of electromagnetic scattering over a large bandwidth in a single measurement, direct detection of the electric field, impulse excitation of targets.

46. Dorney, T.; Johnson, J.; Mittleman, D.; Baraniuk, R.; **"Imaging with THz pulses"** International Conference on Image Processing, 2000. Proceedings. 2000, Volume: 1 , Pages:764 – 767, 10-13 Sept. 2000.

One of the early articles that demonstrate a real-time imaging system based on terahertz (THz) time-domain spectroscopy. It states that this technique offers a range of unique imaging modalities due to the broad bandwidth, sub-picosecond duration, and phase-sensitive detection of the THz pulses. This paper provides an introduction of the state-of-the art in THz imaging. This article also explores in brief an interferometric arrangement to provide a background-free reflection imaging geometry. The second applies novel digital signal processing algorithms to extract useful information from the THz pulses. The possibility exists to combine spectroscopic characterization and/or identification with pixel-by-pixel imaging.

47. Brucherseifer, M.; Pellemans, H.P.M.; Haring Bolivar, P.; Kurz, H.; **"THz spectroscopy with ultrahigh sensitivity"** Conference on Lasers and Electro-Optics, 2000., Pages:553 – 554, 7-12 May 2000.

Shows a new method to enhance the sensitivity of THz spectroscopy to relative changes of 10^{-10} in intensity by shaking a sample through the focus of a THz beam and using lock-in detection on the shaking frequency. Since the signal-to-noise ratio is mostly restricted to 10^4 to 10^6 in intensity. Especially for thin films of material the absorption and time delay of a THz pulse are mostly too low to be detected.

48. Nemec, H.; Kuzel, P.; Khazan, M.; Sch, S.; Wilke, I.; **"Study of carrier dynamics in LT GaAs by means of time-resolved emission terahertz spectroscopy"** International Quantum Electronics Conference, 10-15 Sept. 2000 .

The experimental setup explained in this paper used 80 fs laser pulses at 800 nm generated by a self-mode-locked Ti:sapphire laser to excite biased GaAs samples. Several samples characterised by different deposition temperatures ranging between 175 and 250/spl deg/C were studied. The irradiated THz waveform was measured using a ZnTe electro-optic sensor (without any focusing optics to avoid the waveform reshaping). The THz signal was studied as a function of several parameters (applied voltage, pump laser intensity, distance between biased electrodes). Lateral scans of the emitter position (with regard to the pump beam) were also performed.

49. D. D. Arnone, C. M. Ciesla, S. Egusa, M Pepper, J.M. Chamberlain, C Bezant, E. H. Linfield, R Clothier, and N Khammo: " Applications to Terahertz (THz) Technology to Medical Imaging" EUROPTO Conference on Terahertz Spectroscopy and Applications II, Munich, Germany, SPIE Vol. 3828, pages 209 – 219, June 1999.

50. Chen, Q.; Zhiping Jiang; Xu, G.; Zhang, X.-C.; **"Applications of terahertz time-domain measurement on paper currencies"** The Pacific Rim Conference on Lasers and Electro-Optics, 1999. CLEO/Pacific Rim '99., Volume: 2 , Pages:547 – 548, 30 Aug.-3 Sept. 1999.

Explains the theory that time-domain measurement of a THz pulse provides an alternative method for the dollar bill thickness characterization with an unparalleled data acquisition rate.

51. Zhiping Jiang; Zhang, X.-C.; **"THz imaging via electro-optic effect"** Microwave Symposium Digest, 1999 IEEE MTT-S International , Volume: 3 , Pages:941 – 944, 13-19 June 1999.

Discusses three electro-optic based terahertz imaging systems: the point scanning system, a two-dimensional charge-coupled device (CCD) system and a one-dimensional spatio-

temporal chirped pulse imaging system. A complete comparison between the scanning system and CCD systems is given with explanation about the CCD systems that provide high acquisition speed by taking unique advantage of parallel measurement. Possible improvements are also discussed.

52. Han, P.Y.; Cho, G.C.; Zhang, X.-C.; **"Mid-infrared THz imaging"** Summaries of Papers Presented at the Conference on Lasers and Electro-Optics, 1999. CLEO '99., 23-28 May 1999.
Reports on THz imaging with a high spatial and temporal resolution using a free-space electro-optic sampling technique in the mid-infrared frequency range. A spatial resolution of sub 70-μm is achieved. This technique enables to demonstrate the time-resolved THz trans-illumination for imaging of biological cells. Results demonstrate that the feasibility of THz imaging of biological tissue with a sub 70-micron spatial resolution and sub 100-fs temporal resolution.

53. Zhiping Jiang; Xi-Cheng Zhang; **"Terahertz imaging via electrooptic effect"** IEEE Transactions on Microwave Theory and Techniques, , Volume: 47 , Issue: 12 , Dec. 1999, Pages:2644 – 2650.
Describes three of the electro-optic based THz imaging systems: the point scanning system, 2D CCD system and 1D spatio-temporal chirped pulse imaging system. The comparisons between the scanning system and CCD systems are given. The paper emphasizes on the CCD systems which provide high acquisition speed by taking the unique advantages of parallel measurement. Improvements in these techniques are also discussed.

54. Nuss, M.C., "Terahertz waves, T-rays, and T-birds", Summaries of papers presented at the Conference on Lasers and Electro-Optics, 1998. CLEO 98. Technical Digest, 3-8 May 1998.

55. Mittleman, D.M.; Neelamani, R.; Baraniuk, R.G.; Nuss, M.C.; "Applications of terahertz imaging" Nonlinear Optics '98: Materials, Fundamentals and Applications Topical Meeting, Pages: 294 – 296, 10-14 Aug. 1998.

56. 1998 IEEE Sixth International Conference on Terahertz Electronics Proceedings. THZ 98. (Cat. No.98EX171 IEEE Sixth International Conference on) Terahertz Electronics Proceedings, 1998. THz Ninety Eight. 1998, 3-4 Sept. 1998.

57. Eloy, J.-F.; Gerbe, V.; Trombert, J.-H.; Wilhelmsson, H.; **"Pump and probe experimental setup with opto-electronically pulsed antenna for giga/terahertz spectroscopy"**

Instrumentation and Measurement, IEEE Transactions on , Volume: 47 , Issue: 2 , April 1998 Pages:453 – 458.

Presents a detailed description of a picosecond pump–probe optoelectronic pulsing (generating electromagnetic transients in free space) and sampling system. This system will be used for spectroscopy in a [10–100]-GHz range of materials such as semiconductors. The signal-to-noise ratio obtained in this system is greater than 40 dB and the time resolution can be less than 500 fs, thereby permitting studies of very fast, low-amplitude transient phenomena.

58. Wynne, K.; **"Time-Resolved Terahertz Spectroscopy of Condensed Reactions"** European Quantum Electronics Conference, 1998. 1998 EQEC., 14-18 Sept. 1998.

Brief review of a system developed for ultra fast visible/near-UV pump, THz-probe spectroscopy. Pump-probe experiments were performed on the carrier dynamics of photoexcited SI GaAs and the dynamic dipole solvation of two different dyes in polar solution.

59. Zhang, X.-C.; "**THz beam sensors**" Summaries of papers presented at the Conference on Lasers and Electro-Optics, 1998. CLEO 98. Technical Digest. , 3-8 May 1998.

This article (containing only the summary) states that the use of thin ZnTe electro-optic sensors for coherent characterization of a freely propagating terahertz beam demonstrated a bandwidth up to 37 THz. This represents a significant improvement over the 7 THz bandwidth by using a GaP crystal, and also confirms the broadband nature of mid-IR radiation generated by optical rectification. With the ultra short laser pulses of 10 fs, it is feasible to generate and detect a THz beam with a bandwidth over 40 THz.

60. Lubecke, V.M.; Mizuno, K.; Rebeiz, G.M.; "**Micromachining for terahertz applications**", IEEE Transactions on Microwave Theory and Techniques, Volume: 46 , Issue: 11 , Pages:1821 – 1831, Nov. 1998.

Presents an overview of recent progress in the research and development of micromachined antennas, transmission lines, waveguides structures, and planar movable components for terahertz frequencies. Micromachining is shown to provide a low-cost alternative to conventional machined-waveguide technology, resulting in antennas with excellent radiation patterns, low-loss tuners, and three-dimensional (3-D) micromachined structures suitable for terahertz applications. Fabrication procedures for a variety of micromachined waveguide and planar structures are described here, along with measured terahertz performance. Applications of micromachining techniques for terahertz systems include focal-plane imaging arrays

requiring a large number of elements and low-cost receivers for commercial and industrial applications such as pollution monitoring.

61. Zhiping Jiang; Sun, F.G.; Zhang, X.-C.; **"Spatio-temporal imaging of THz pulses"** IEEE Sixth International Conference on Terahertz Electronics Proceedings, 1998. THz Ninety Eight. 1998, Pages: 94 – 97, 3-4 Sept. 1998.

Reports the use of an optoelectronic system for the measurement of THz pulses by use of chirped pulse technology. This system measures the spatio-temporal distribution of a free-space pulsed radiation with an unprecedented data acquisition rate. Acquisition of picosecond THz field pulses without using mechanical time-delay devices has been achieved. A single-shot electro-optic measurement of the temporal waveform of a THz pulse has been demonstrated.

62. IEE Colloquium on Terahertz Technology and its Applications (Ref. No.1997/151) IEE Colloquium on Terahertz Technology and Its Applications (Digest No: 1997/151), 10 April 1997.

63. Hunsche, S.; Koch, M.; Brener, I.; Nuss, M.C.; **"THz imaging in the near-field"** Summaries of Papers Presented at the Conference on Lasers and Electro-Optics, 1997. CLEO '97., , Volume: 11 , Pages:64 – 65, May 18-23, 1997.

Explains a demonstration of near-field imaging to create high-resolution "T-ray" image. A small aperture is inserted in the focus of the imaging system described in B. B. Hu and M. C. Nuss, Opt. Lett. 20, 1716 (1995). The experiment uses a tapered metal tube with a small, circular exit aperture. Due to the larger focal diameter for the low-frequency components of the THz pulses and their larger diffraction losses after passing the aperture the transmission through the aperture is strongly frequency dependent. This results in a spectral narrowing and to the observed the changes of the THz waveform towards a more oscillating structure. This paper concludes by stating that the improved resolution is indeed a near-field effect.

64. Nuss, M.C.; "Chemistry is right for T-ray imaging" IEEE Circuits and Devices Magazine, Volume: 12, , Issue: 2 , Pages:25 – 30, March 1996.

Exploratory article at the infancy of THZ imaging.

65. Daniel M. Mittleman, Rune H. Jacobsen and M. C. Nuss: "**T-ray imaging**", IEEE Journal of Selected topics in Quantum Electronics, Vol. 2, No Pages: 679 – 692, (3 September 1996).

Describes various technologies and techniques necessary to perform terahertz imaging. Characteristics of T-ray for chemical imaging are explained. A generalized T-ray imaging

setup with descriptive information of the components of the setup such as laser source, optoelectronic switches, beam optics and signal acquisition is also provided in this article. Various commercial applications such as T-ray imaging for moisture, quality control, and tomography are explained in brief along with the time domain and wavelet based analysis of the T-rays.

66. Q.Wu, D. Hewitt and X. –C. Zhang: “Two dimensional electro-optic imaging of THz beams”, Applied Physics Letters, 69(8), pages 1026 – 1028, (19 August 1996).